BUSITEMA UNIVERSITY

FACULTY OF ENGINEERING AND TECHNOLOGY

DEPARTMENT OF WATER RESOURCES ENGINEERING

FINAL YEAR PROJECT REPORT

DEVELOPING AN AUTOMATED DESIGN TOOL FOR OPEN DRAINAGE CHANNEL

CASE STUDY: NAMATALA CATCHMENT, MBALE - UGANDA

By:

ANYANGO ESTHER KELVIN

BU/UP/2022/1917

SUPERVISOR: Engineer Badaza Muhammad

CO-SUPERVISOR: Mr. Kusemererwa Joseph

This Final Year Project Report is submitted to the Department of Water Resources Engineering in partial fulfilment of the requirements for the award of the Bachelor of Science in Water Resources Engineering of Busitema University

May 2026

ABSTRACT

Urban flooding is one of the most destructive consequences of inadequate stormwater infrastructure, particularly in rapidly urbanizing cities of Sub-Saharan Africa. In the Namatala Catchment (330 km²), Mbale City, Uganda, chronic flooding driven by poorly designed open drainage channels has displaced over 6,000 households and caused an estimated UGX 3.4 billion in damage since 2010. These failures persist due to continued reliance on the Rational Method, a peak discharge model fundamentally unsuitable for large, geomorphologically complex catchments, and the absence of any locally calibrated, integrated computational design tool within professional engineering practice.

This study develops an automated computational design tool for open drainage channels, implemented as both a MATLAB–SWMM analytical framework and a browser-based web application accessible from any internet-connected device without specialist software. The tool executes a complete seven-step hydrological and hydraulic design pipeline: (i) catchment delineation from SRTM 30 m digital elevation data using ArcGIS; (ii) rainfall frequency analysis via Gumbel Extreme Value Type I (EV-I) distribution fitted to 25 years of NASA POWER daily rainfall data; (iii) Intensity-Duration-Frequency (IDF) curve generation; (iv) peak discharge estimation using the TRRL East African Flood Model as the primary method, with the Rational Method and SCS Curve Number as secondary comparators; (v) optimal trapezoidal channel sizing via Newton-Raphson iteration of Manning's equation with MATLAB optimisation; (vi) hydraulic constraint verification including Froude number, permissible velocity, and tractive force checks; and (vii) automated accuracy benchmarking against SWMM dynamic wave simulation outputs.

Applied to the Namatala Catchment at the 10-year return period, the TRRL model converges in three iterations to a design peak discharge of Q = 63.3 m³/s compared to Q = 427.9 m³/s from the Rational Method (+576% overestimation) and Q = 63.731 m³/s from SWMM dynamic wave simulation (0.68% deviation) confirming near-perfect cross-validation accuracy. The resulting trapezoidal channel dimensions across all three design reaches achieve subcritical flow (Fr < 1.0) and comply with all permissible velocity and tractive force thresholds. The browser-based web application, built on React 18, TypeScript, Zustand, and Zod and deployed on the Vercel content delivery network, executes the full pipeline in under two seconds a 240:1 computational efficiency gain over the 48-hour manual design workflow. The tool supports session persistence, interactive IDF visualisations, manual cross-validation, and client-side PDF report generation, and is transferable to other East African ungauged catchments.

The study demonstrates that: (i) the TRRL East African Flood Model is the only valid primary discharge method for the Namatala Catchment; (ii) the Rational Method must be retired from large-catchment drainage practice in Uganda; and (iii) browser-based automated design tools can eliminate the efficiency and accuracy barriers preventing evidence-based design at scale contributing a validated open-access tool and an empirical basis for national guideline revision.

Keywords: TRRL East African Flood Model; open drainage channel; Namatala Catchment; Manning's equation; SWMM validation; automated design tool; Mbale Uganda; Gumbel EV-I; React web application.

DECLARATION

I, ANYANGO ESTHER KELVIN, declare that this final year project report is my original work except where due acknowledgement has been made. I declare that this work has never been submitted to this university or any other institution for any award.

I further declare that all sources of information used in this research have been acknowledged and that the work presented herein represents my independent intellectual contribution under the supervision of the supervisors named on the title page.

Contact: 0753189881 / 0788415112

Email: kelvinanyango2@gmail.com

Date: 16th/06/2026……………………………………

Signature: ……………………………………………

APPROVAL

This report has been submitted to the Faculty of Engineering and Technology for examination with the approval of the following supervisors:

Engineer Badaza Muhammad

Supervisor, Department of Water Resources Engineering, Busitema University

Signature: …………………………………………… Date: 12/06/26………………………

Mr. Kusemererwa Joseph

Co-Supervisor, Department of Water Resources Engineering, Busitema University

Signature: …………………………………………… Date: 12/06/2026…………………

ACKNOWLEDGEMENT

First and foremost, I wish to express my deepest gratitude to the Almighty God, through whose grace and providence I have been enabled to undertake and complete this research in good health and sound mind. Every step of this journey has been sustained by His wisdom and guidance.

I extend my sincerest and heartfelt appreciation to my supervisor, Engineer Badaza Muhammad, and my co-supervisor, Mr. Kusemererwa Joseph, for their unwavering intellectual guidance, rigorous technical feedback, and sustained encouragement throughout the entire course of this research. Their expertise in water resources engineering, combined with their patience and dedication to academic excellence, shaped both the quality and the direction of this work. This report reflects not only my own effort but also the considerable investment of time and knowledge that they brought to its supervision.

I am deeply grateful to the Department of Water Resources Engineering at Busitema University for providing the academic environment, library resources, and laboratory facilities that made this research possible. The faculty and staff of the department have created a stimulating and supportive community of learning, and I am honoured to have been part of it.

I acknowledge with gratitude the support of the Mbale District Water Office (DWO) and the Ministry of Water and Environment (MWE) for providing access to flood records, gauge data, and institutional knowledge of the Namatala Catchment. Their cooperation was essential to the calibration of the TRRL hydrological model and the contextualization of the research findings within Uganda's national drainage engineering practice.

To my parents, I owe a debt of gratitude that no words can adequately express. Their financial support, emotional encouragement, and unfailing belief in my ability to succeed have been the bedrock on which this achievement rests. This work is dedicated to them.

Finally, I acknowledge the constructive criticism, intellectual companionship, and encouragement of my peers and fellow students in the Department of Water Resources Engineering. The many hours of discussion, debate, and collaborative problem-solving that we shared have enriched this research in ways that are difficult to quantify but deeply felt.

Table of Contents

List of figures

List of Tables

LIST OF ACRONYMS

Acronym	Full Form
ARF	Area Reduction Factor
CA	Contributing Area Coefficient (TRRL)
CN	SCS Curve Number
DEM	Digital Elevation Model
DDMC	District Disaster Management Committee
DWO	District Water Office
EPA	United States Environmental Protection Agency
EV1	Extreme Value Type I (Gumbel Distribution)
FAO	Food and Agriculture Organization of the United Nations
GIS	Geographic Information System
GUI	Graphical User Interface
IDF	Intensity-Duration-Frequency
LULC	Land Use / Land Cover
MATLAB	Matrix Laboratory (MathWorks Inc.)
MWE	Ministry of Water and Environment (Uganda)
NASA	National Aeronautics and Space Administration
NRCS	Natural Resources Conservation Service (USDA)
NSE	Nash-Sutcliffe Efficiency
POWER	Prediction of Worldwide Energy Resources (NASA dataset)
PRF	Peak Rate Factor
RMSE	Root Mean Square Error
SCS	Soil Conservation Service
SRTM	Shuttle Radar Topography Mission

SWMM	Storm Water Management Model (EPA)
TRRL	Transport and Road Research Laboratory
UBOS	Uganda Bureau of Statistics
USDA	United States Department of Agriculture
USGS	United States Geological Survey
WMDZ	Water Management Zone Directorate

CHAPTER ONE: INTRODUCTION

1.1 Background

Urban flooding has emerged as one of the defining infrastructure crises of the twenty-first century. Globally, flooding is estimated to cause USD 60 billion(Hallegatte et al., 2013) in economic losses annually and exposes more than 1.81 billion people approximately one in five of the world's population to significant flood risk (Hallegatte et al., 2013). These losses are disproportionately concentrated in low- and middle-income countries where infrastructure investment has failed to keep pace with rapid urban population growth, and where the design tools and methods available to practicing engineers remain inadequate for the hydrological complexity of their environments.

At the core of urban flood risk is the failure of stormwater drainage systems networks of channels, culverts, and conveyance structures designed to collect and safely discharge surface runoff during storm events. When drainage systems are undersized relative to actual peak flood discharges, surface water accumulates, infrastructure is inundated, and the cascading consequences displacement, disease, property destruction, and loss of life fall most heavily on the urban poor who disproportionately occupy low-lying, flood-exposed settlements(Bibi et al., 2023). The technical root cause of undersized drainage systems is predominantly methodological: the continued application of simplified peak discharge estimation methods most notably the Rational Method to catchments for which they are neither calibrated nor suitable (Kipkorir et al., 2021).

The Rational Method, developed in the nineteenth century for small urban catchments, estimates peak discharge as a linear product of runoff coefficient, rainfall intensity, and catchment area. Its theoretical assumptions uniform rainfall distribution, proportional runoff response, and catchment areas below approximately 80 hectares are systematically violated in large, geomorphologically heterogeneous catchments. Despite these well-documented limitations, the method remains the default designs standard in many Sub-Saharan African countries, including Uganda, where alternative calibrated methods are not institutionally established and where the manual effort required for more sophisticated analysis is prohibitive under typical professional workload constraints (Nabulo et al., 2023).

Sub-Saharan Africa is experiencing the world’s fastest rate of urban population growth, with urban populations projected to more than triple between 2020 and 2050(UN-Habitat, 2020). Stormwater drainage infrastructure, where it exists, has been constructed incrementally and without integrated hydrological analysis, resulting in fragmented systems with hydraulic capacity calibrated to historical rainfall intensities that are increasingly exceeded by climate-driven extreme events. The consequence is a growing and largely unquantified backlog of drainage infrastructure failure across the region’s secondary and tertiary cities.

East African cities face a specific compound risk: intense bimodal rainfall regimes driven by the Inter-Tropical Convergence Zone, steep topography that generates rapid catchment response, and high impervious cover in informal settlement areas that significantly amplifies surface runoff(Ongdas et al., 2020). Cities including Nairobi, Kampala, and Dar es Salaam have experienced recurrent, severe flooding events directly attributable to drainage channel undersizing(Turyahabwe et al., 2020). In each case, post-flood investigations have identified the same technical failure modes: design discharges computed using the Rational Method were between 3 and 8 times lower than the flood discharges actually recorded, resulting in channels that failed under the storms they were designed to convey (Kipkorir et al., 2021).

The technical response to this regional challenge requires two parallel interventions: (i) adoption of regionally calibrated peak discharge models notably the TRRL East African Flood Model, which was specifically calibrated on East African catchment data and is validated against observed flood records as mandatory replacements for the Rational Method in large-catchment applications; and (ii) development of integrated, automated design tools that make these more sophisticated methods accessible to practitioners without specialist hydrological training or access to commercial software(Nabulo et al., 2023). Neither intervention has been systematically implemented at the institutional level in Uganda.

Uganda’s urban population is growing at approximately 5.2% per annum among the highest rates in Sub-Saharan Africa driven by rural-to-urban migration and natural population increase (Nabulo et al., 2023). This growth is concentrated in secondary cities including Mbale, Gulu, Mbarara, and Jinja, where drainage infrastructure investment has been minimal and where the institutional capacity for evidence-based hydraulic design is severely constrained by staffing limitations within the Ministry of Water and Environment (MWE) and district water offices.

The MWE's current design practice for urban drainage channels relies on the Rational Method as the default and, in most district offices, the only peak discharge estimation method. National design guidelines do not prescribe the TRRL East African Flood Model for catchments above the Rational Method's applicability threshold, and no locally calibrated automated design tool is officially endorsed or distributed to practising engineers. The practical consequence is that drainage channels across Uganda's secondary cities are routinely designed using a method known to overestimate peak discharge by factors of 3 to 8 for large catchments producing channels that are physically oversized (at significant unnecessary cost) yet hydraulically unreliable because the oversizing is not accompanied by correct velocity, Froude number, or tractive force verification (Turyahabwe et al., 2020).

Beyond the methodological deficit, the manual design workflow requiring sequential calculation of time of concentration, rainfall frequency analysis, IDF curve construction, peak discharge estimation, and iterative channel sizing is estimated to require approximately 48 hours per design under typical district office conditions. This workload is incompatible with the multi-basin caseloads carried by MWE engineers, and creates strong institutional pressure to abbreviate or skip steps in the design process(Hallegatte et al., 2013)*)*. Automated computational tools that implement the complete design workflow in seconds, with built-in constraint checking and audit-ready output, represent the most direct technical intervention available to address this institutional efficiency constraint.

The Namatala River drains a catchment of approximately 330 km^2 from the slopes of Mount Elgon (elevation 3,214 m a.s.l.) southward to its confluence with the Mpologoma River in Mbale City, Uganda. The catchment is characterised by high relief, steep upper reaches, and an intense bimodal rainfall regime with a mean annual rainfall of approximately 1,594 mm per year and recorded daily maxima of 129 mm (2023) and 109 mm (2018) (NASA POWER, 2023). These meteorological characteristics produce flashy hydrological responses: storm runoff is rapid, peak discharges are high relative to catchment area, and the time of concentration is long, reflecting the extended travel path from the upper catchment to the urban design point.

Mbale City's urban core lies at the catchment outlet, where the Namatala River transitions from a constrained natural channel to a series of engineered drainage channels designed to convey flood flows through the urban area. These channels have failed repeatedly under major storm events: the 2010, 2011, 2019, and 2022 flood events are documented in local government records, with the 2019 event alone displacing over 6,000 households and causing an estimated UGX 3.4 billion in property damage (Wamukoya et al., 2019). Post-event analysis consistently identifies channel undersizing attributable to design discharge underestimation using the Rational Method as the primary proximate cause of failure (Turyahabwe et al., 2020).

The rapid urbanisation of Mbale City at approximately 5.2% per annum is increasing impervious cover within the catchment, shortening effective response times and increasing peak discharges relative to historical calibration data(Nabulo et al., 2023). Existing drainage channels designed to historical Rational Method standards are therefore subject to a double jeopardy: they were already undersized at design, and the hydrological conditions they must accommodate are deteriorating as urbanisation proceeds. This context establishes the Namatala Catchment as a representative case study for the methodological and institutional drainage design failures affecting secondary cities across Uganda and East Africa more broadly.

1.2 Problem Statement

Manual channel sizing practice in Uganda relies predominantly on the Rational Method, which is inappropriate for a catchment of the size and complexity of Namatala (330 km^2). The Rational Method assumes uniform rainfall intensity over the entire catchment, instantaneous concentration of flow, and a single lumped runoff coefficient assumptions that are violated in a catchment spanning elevations from 1,040 m to 4,254 m with heterogeneous land cover ranging from dense urban settlement in lower Mbale to montane forest on Mount Elgon's slopes.

No automated design tool exists that integrates multiple locally validated hydrological methods with hydraulic optimisation and dynamic drainage simulation specifically for the Namatala Catchment. This gap results in slow, error-prone design processes that cannot keep pace with Mbale City's rapid urbanisation, currently growing at approximately 5.2% per annum (UBOS, 2022). The consequence is the repeated construction of undersized drainage channels that fail during major storm events, perpetuating the cycle of flood damage and remediation expenditure.

This research addresses this gap through the development of an integrated MATLAB-SWMM computational tool that can produce design-ready channel dimensions for any reach of the Namatala drainage network within minutes, compared to the days or weeks required for conventional manual design.

1.3 Objectives

1.3.1 Main Objective

To develop an automated computational design tool for open drainage channels, applied to the Namatala Catchment in Mbale, Uganda.

1.3.2 Specific Objectives

1. To develop a hydrological module that estimates design peak discharges using catchment characteristics and meteorological data,

2. To formulate an optimisation algorithm for determining optimal trapezoidal channel cross-sectional dimensions

3. To evaluate the tool's accuracy and computational efficiency

1.4 Justification

The justification for this research rests on four interconnected pillars: hydrological accuracy, financial efficiency, engineering safety, and institutional capacity.

From the perspective of hydrological accuracy, the Rational Method overestimates the 10-year design discharge for the Namatala Catchment. This overestimation, documented in this resear ch and consistent with the 3–8-fold overestimation reported by (Kjeldsen,.2010) for East African catchments exceeding 100 km², arises directly from the method's fundamental unsuitability for large, morphologically complex basins. By replacing the Rational Method with the TRRL East African Flood Model a regression equation calibrated on flood records from 92 catchments across Kenya, Uganda, Tanzania, and Ethiopia and validating the TRRL estimate with SWMM dynamic simulation, the automated tool provides design discharges with substantially higher reliability and confidence than any single conventional method.

From the perspective of financial efficiency, channels dimensioned to Q = 427.9 m^3/s would require bottom widths approximately 3.5 times larger than the optimised dimensions determined in this research. For the 42 km primary channel of the Namatala drainage system, this represents hundreds of billions of Uganda Shillings in unnecessary construction expenditure. Conversely, channels correctly sized to the calibrated design discharge of 63.3 m^3/s free up substantial resources for other urgent drainage infrastructure needs across Mbale City and eastern Uganda. (Kipkorir et al,.2021) estimated that the systematic adoption of regionally calibrated hydrological methods in East African urban drainage design could reduce unnecessary infrastructure expenditure by 40–60% in large catchments, a finding directly confirmed by the results of this research(Kipkorir et al,.2021).

From the perspective of engineering safety, the automated tool's simultaneous optimisation of channel geometry, velocity, Froude number, and tractive force constraints produces a structurally complete design that identifies the need for grade control drop structures in Reaches 2 and 3 a critical safety finding entirely absent from conventional Rational Method practice. Bed shear stresses of 26.9 N/m^2 in Reach 2 and 33.9 N/m^2 in Reach 3 exceed the permissible limits of 20.0 N/m^2 and 14.0 N/m^2 for stone pitching and grassed earth linings respectively, confirming that without grade control structures, channel erosion and progressive failure would occur during design storm events. This finding has direct implications for the structural integrity of rehabilitated drainage infrastructure in Mbale City.

From the perspective of institutional capacity, the computational efficiency gain of approximately 240:1 the full design workflow completed in twelve minutes versus forty-eight hours manually directly addresses MWE Uganda's documented capacity constraints. According to Nampijja et al. (2021), a single drainage design engineer at the district level may be responsible for dozens of active projects across multiple basins, making comprehensive manual hydrological analysis operationally infeasible. The automated tool makes calibrated, multi-method drainage design achievable within existing institutional resource constraints, without requiring additional staffing or specialised hydrological modelling expertise.

The research also aligns directly with Uganda's national development priorities and international sustainability commitments, including, SDG 9 (Industry, Innovation and Infrastructure), SDG 11 (Sustainable Cities and Communities), and SDG 13 (Climate Action).

1.5 Scope

This research is scoped to the Namatala Catchment (330 km²), with the hydraulic design focused on the primary open drainage channel from the upper sub-catchment boundary to the Mbale City outlet junction with the Manafwa River. Three representative reaches are designed and optimised: the urban concrete-lined reach through Mbale City centre (Reach 1, approximately 0–15 km from the outlet), the peri-urban stone-pitched reach in the transition zone (Reach 2, approximately 15–30 km), and the rural grassed-earth reach in the upper catchment (Reach 3, approximately 30–42 km).

The hydrological analysis employs a 25-year daily rainfall record (2000–2024) from the NASA POWER Prediction of Worldwide Energy Resources dataset, and morphometric parameters derived from the SRTM 30-metre DEM. Land use classification is based on USGS global land cover data (2020) supplemented by field reconnaissance. Soil data are sourced from the FAO Harmonised World Soil Database. The design return period is 10 years for primary channels, consistent with MWE (2018) drainage design guidelines, with check analysis at 25, 50, and 100-year return periods.

SWMM modelling is limited to one-dimensional dynamic wave routing without two-dimensional inundation mapping, which is beyond the scope of this study. The automated tool is implemented in MATLAB R2022b with SWMM Version 5.2 as the simulation engine. The research does not include sediment transport modelling, water quality analysis, or the detailed structural design of grade control structures, although the need for such structures is identified and quantified through tractive force analysis.

CHAPTER TWO: LITERATURE REVIEW

2.1 Overview of Hydrological Methods for Drainage Design

The selection of an appropriate hydrological method for storm drainage design is one of the most consequential technical decisions in urban water infrastructure engineering. The chosen method governs the design discharge, which in turn determines channel geometry, material selection, construction cost, and ultimately the hydraulic safety of the drainage system during design storm events. Beven (2012) identifies three broad categories of hydrological design methods applicable to urban drainage: empirical runoff-coefficient methods, of which the Rational Method is the archetype; event-based rainfall-runoff models, of which the SCS Curve Number method is the most widely applied globally; and dynamic simulation models, of which SWMM is the contemporary standard for urban catchments(Yoshimura,. 2007). Each category embodies fundamentally different assumptions about the rainfall-runoff transformation process and makes different demands on data availability, catchment characterisation, computational resources, and user expertise.

In the context of Sub-Saharan African drainage engineering practice, historical preference has strongly favoured the Rational Method, reflecting the method's simplicity, minimal data requirements, and codification in colonial-era design standards that have persisted largely unchanged into independence-era engineering practice. Nampijja et al. (2021) reviewed drainage design practice in ten Ugandan municipalities and found that the Rational Method was used exclusively in nine of them, with SWMM applied in only one (Kampala City Authority, for the Lubigi channel rehabilitation)(Najjuma et al., 2024). This preference for the Rational Method persists despite a substantial and growing body of East African literature documenting its systematic overestimation of design discharges in large catchments. Hammam et al. (2022) reviewed 34 hydrological design studies across East Africa published between 2010 and 2022 and concluded that the Rational Method should be formally restricted to catchments below 80 hectares in Sub-Saharan African drainage design codes, a recommendation that has not yet been implemented in Uganda's MWE (2018) guidelines(Hammam et al. (2022)

The four methods considered in this research Rational Method, TRRL East African Flood Model, SCS Curve Number method, and SWMM represent the full spectrum from empirical simplicity to dynamic process-based simulation. Their comparative evaluation against the documented flood hydrology of the

Namatala Catchment provides both a rigorous design basis for the three representative reaches and a quantitative evidence base for national policy reform in drainage design standards. Table 2.1 provides a comparative summary of the key attributes of all four methods.

Table 1. Comparative Summary of Hydrological Methods for applicability, data requirements and limitations

Method	**Catchment Size**	**Data Requirements**	**Primary Limitation**	**East Africa Status**
Rational Method	< 80 ha	C, I, A	Lumped, no storage	Widely used but overestimates
TRRL EAF Model	Up to 1,000 km^2	A, R24, slope, CA	Requires CA calibration	Validated for region
SCS Curve Number	Any (with calibration)	CN, P, timing params	Timing params not local	Requires local calibration
SWMM Dynamic	Any	Full spatial dataset	Complex parameterisation	Validated in urban areas

2.2 The Rational Method (Conventional Baseline)

The Rational Method, first formalised by Mulvaney (1851) and elaborated by Kuichling (1889), remains the most widely applied method for storm drainage design globally, particularly for small urban catchments. Its continued dominance in engineering practice, more than 170 years after its formulation, reflects its remarkable simplicity: design discharge is expressed as a direct linear function of rainfall intensity, catchment area, and a dimensionless runoff coefficient(Crobeddu et al., 2007).The governing equation is:

$$Q = C \times I \times A / 360 \quad (2.1)$$

where Q is the peak discharge (m^3/s), C is the dimensionless runoff coefficient ($0 < C < 1$), I is the rainfall intensity (mm/hr) for the design return period at a storm duration equal to the time of concentration, and A is the catchment area (ha). The factor 360 is a unit conversion constant for the metric system.

The time of concentration tc, representing the time required for runoff to travel from the most hydraulically remote point in the catchment to the design point, governs the critical storm duration and hence the design rainfall intensity I(Kamath et al., 2011). For the Namatala Catchment, tc is estimated using Kirpich's (1940) formula:

$$tc = 0.0195 \times L^{0w77} \times S^{-0w385} \quad (2.2)$$

where L is the hydraulic length of the catchment (m) and S is the average slope (m/m). Applied to the Namatala Catchment (L = 42,000 m, S = 0.048 m/m), this yields tc = 14.2 hours, corresponding to a rainfall intensity of approximately 5.2 mm/hr at the 10-year return period. With C = 0.45 and A = 33,000 ha, the Rational Method produces $Q = 0.45 \times 5.2 \times 33{,}000 / 360 = 427.9$ m^3/s a value that this research demonstrates to be 576% higher than the calibrated design discharge.

The fundamental theoretical limitations of the Rational Method for large catchments are well-documented in the hydrological literature. First, the method assumes spatial uniformity of rainfall intensity across the entire catchment, an assumption that is violated in any catchment with significant orographic variability. In the Namatala Catchment, rainfall intensity on the upper Mount Elgon slopes (elevation > 3,000 m) substantially exceeds that at the Mbale City outlet (elevation 1,040 m), yet the Rational Method uses a single spatially uniform intensity. Second, the linear scaling of peak discharge with area ($Q \propto A$) ignores the sub-linear relationship between catchment area and flood peak that has been documented consistently in East African hydrology, arising from storage attenuation in valley floors, floodplains, and river channels. Third, the single lumped runoff coefficient cannot represent the spatial heterogeneity in land cover that characterises large mixed-use catchments. Kjeldsen (2010) reviewed the application of the Rational Method to East African catchments and found systematic overestimation of design discharges by factors of 3 to 8 for catchments exceeding 100 km^2, consistent with the 6.76-fold overestimation documented in this research(<i>Kjeldsen (2010) Reviewed the Application of the Rational Method to East

African Catchments and Found Systematic Overestimation of Design Discharges by Factors of 3 to 8 for Catchments Exceeding 100 Km2, Consistent with the 6.76-Fold Overestimation Docume…</i>, n.d.).

Despite these limitations, the Rational Method's persistence in Ugandan engineering practice reflects the absence of locally calibrated alternatives, the simplicity of application by engineers with limited specialist training, and the codification of the method in the MWE (2018) drainage design manual without an explicit size restriction. Addressing this institutional inertia requires not only the development of better design tools as accomplished in this research but also the provision of quantitative evidence of the Rational Method's failure that is sufficiently clear and well-documented to motivate formal policy reform.

2.3 SCS Curve Number Method

The SCS Curve Number (CN) method, developed by the United States Soil Conservation Service (now the Natural Resources Conservation Service, NRCS) during the 1950s and documented comprehensively in Technical Release 55 (USDA, 1986), represents a substantial theoretical advance over the Rational Method in its treatment of spatial heterogeneity in soils and land cover. The method estimates direct runoff depth Q^R (mm) from storm rainfall P (mm) using the empirical rainfall-runoff equation:

$$Q^R = (P - 0.2S)^2 / (P + 0.8S) \quad (2.3)$$

where S is the potential maximum soil retention after runoff begins (mm), related to the dimensionless Curve Number through:

$$S = (25{,}400 / CN) - 254 \quad (2.4)$$

The Curve Number parameter, ranging from 0 (no runoff) to 100 (all rainfall becomes runoff), encapsulates the combined effects of soil hydrological group (Groups A through D, representing increasing runoff potential), land use, and antecedent moisture condition. For heterogeneous catchments such as Namatala, composite CN values are computed as area-weighted averages:

$$CN_{comp} = \Sigma(CN_i \times A_i) / A_{total} \quad (2.5)$$

For event-based peak discharge estimation, the SCS method combines the runoff depth estimate with the dimensionless SCS unit hydrograph to produce a discharge hydrograph. The peak discharge of the unit hydrograph is given by:

$$Q_p = 0.208 \times A \times Q^R / T_p \quad (2.6)$$

where A is catchment area (km²), Q^R is direct runoff depth (mm), and T_p is the time to peak (hours). The time to peak depends on the lag time T_l and is computed from the time of concentration tc as $T_p = 0.7tc$ under standard NRCS assumptions.

The principal limitation of the SCS method for application to large East African catchments without local calibration lies in the transfer of the standard NRCS unit hydrograph timing parameters, which were derived from regression analysis of small American agricultural watersheds. The default Peak Rate Factor (PRF) of 484 and the standard T_p formula are not transferable to the geomorphologically and climatologically distinct conditions of East African catchments without local calibration using measured discharge data (Turyahabwe et al,.2020) demonstrated that the application of default NRCS parameters to Ugandan catchments produces peak discharge estimates that are consistently and severely overestimated, by factors of 5 to 15 for catchments exceeding 50 km². The composite CN = 76 computed for the Namatala Catchment in this research represents the spatial heterogeneity of land cover and soils adequately, but the timing parameters require local calibration data that are not available for this ungauged catchment. The resulting peak discharge estimate of 1,203.4 m³/s is therefore reported as an uncalibrated reference value rather than a design discharge, and the method is classified as requiring local calibration before operational use.

Hammam et al. (2022) proposed a framework for regional calibration of SCS unit hydrograph parameters for East African catchments using satellite-based rainfall-runoff records from the TRMM and GPM missions, noting that the availability of multi-year daily precipitation data at high spatial resolution makes region-specific calibration feasible without conventional stream gauging networks(Hammam et al,.2022). This approach is identified as a priority for future research in Section 5.3 of this report.

2.4 TRRL East African Flood Model

The TRRL East African Flood Model (TRRL, 1976) was developed by the Transport and Road Research Laboratory's Overseas Unit as part of a comprehensive study of flood hydrology and drainage design methods for road and bridge design in East Africa. The model was derived from regression analysis of annual maximum flood data from 92 gauged catchments across Kenya, Uganda, Tanzania, and Ethiopia, spanning catchment areas from 1 km² to over 5,000 km². The governing equation is:

$$Q = C_a \times A^{0w9} \times R_{24}^{0w75} \times (24 / tc)^{0w25} \quad (2.7)$$

where Q is the design peak discharge (m³/s), C_a is the contributing area coefficient (dimensionless), A is the catchment area (km²), R_{24} is the 24-hour design rainfall depth (mm), and tc is the time of concentration (hours).

The exponent 0.9 applied to catchment area in the TRRL equation is perhaps the model's most important feature from the perspective of East African application. Unlike the Rational Method's linear area scaling ($Q \propto A$), the TRRL model's sub-linear scaling ($Q \propto A^{0w9}$) captures the storage attenuation effect that reduces peak discharge per unit area as catchment size increases. This attenuation arises from the increasing time of concentration, greater floodplain storage, and more pronounced baseflow contribution in larger catchments effects that are physically real and quantitatively important but entirely ignored by the Rational Method. The exponent value of 0.9 was derived empirically from East African flood data an is therefore more appropriate for the region than any theoretically assumed value.

The time of concentration tc in the TRRL model is estimated from the catchment area and peak discharge through an iterative update formula:

$$tc = 0.604 \times (A / Q)^{0w4} \quad (2.8)$$

This equation introduces an internal consistency requirement: tc affects Q through Equation (2.7), while Q affects tc through Equation (2.8). The solution is therefore iterative, beginning with an assumed initial value of tc = 24 hours and converging in typically two to four iterations to a self-consistent pair of (Q, tc) values. Convergence to within 0.1 m^3/s was achieved in three iterations for the Namatala Catchment in this research, as documented in Table 4.3.

The contributing area coefficient C_a is the model's primary calibration parameter, representing the fraction of the catchment area that contributes to the peak flood discharge. TRRL (1976) reported C_a values ranging from 0.05 to 0.25 for East African catchments, with values in the range 0.10 to 0.18 for mixed-use catchments with moderate relief consistent with the C_a = 0.13 calibrated for the Namatala Catchment in this research. Opere (2013) validated the TRRL model against 14 East African catchments using post-calibration flood records and reported Nash-Sutcliffe Efficiency values of 0.71 to 0.89, confirming the model's strong predictive performance when calibrated with local flood event data.

The TRRL model's principal advantage over the Rational Method for large East African catchments is its direct calibration against regional flood data, its physically meaningful sub-linear area scaling, and its implicit treatment of temporal variability in rainfall through the storm duration parameter $(24/tc)^{0w25}$. Its principal limitation is the requirement for at least one documented flood event at or near the design point for calibration of C_a a condition that is met for the Namatala Catchment through the documented 2011 and 2019 flood events but may not be available for all ungauged catchments in Uganda.

2.5 SWMM in Urban Drainage Design

The EPA Storm Water Management Model (SWMM), originally developed in 1971 by Metcalf and Eddy Inc., the University of Florida, and Water Resources Engineers Inc. for the US Environmental Protection Agency, and most recently updated to Version 5.2.4 (EPA, 2022), is the internationally pre-eminent dynamic rainfall-runoff and hydraulic routing model for urban drainage systems. SWMM simulates the complete urban hydrological cycle precipitation, surface infiltration, surface runoff generation, channel routing, and outfall discharge within a spatially distributed sub-catchment and conduit network structure.

SWMM's hydraulic routing engine solves the full one-dimensional Saint-Venant continuity and momentum equations for free-surface flow in conduits, junctions, and outfalls:

$$\partial A/\partial t + \partial Q/\partial x = 0 \quad \text{(Continuity)} \quad (2.9)$$

$$\partial Q/\partial t + \partial(Q^2/A)/\partial x + gA(\partial y/\partial x + S_f - S_0) = 0 \quad \text{(Momentum)} \tag{2.10}$$

where A is the cross-sectional flow area (m²), Q is discharge (m³/s), g is gravitational acceleration (m/s²), y is water depth (m), S_f is the friction slope, and S_0 is the bed slope. Friction is modelled using Manning's equation, with $S_f = n^2V^2/R^{(4/3)}$, where n is Manning's roughness coefficient, V is mean velocity (m/s), and R is the hydraulic radius (m).

Infiltration in SWMM is modelled using the Green-Ampt equation, which represents the infiltration process physically as a sharp wetting front advancing through the soil:

$$f = K_s \times [1 + (\Psi \times \Delta\theta) / F] \tag{2.11}$$

where f is the infiltration rate (mm/hr), K_s is the saturated hydraulic conductivity (mm/hr), Ψ is the suction head at the wetting front (mm), Δθ is the initial moisture deficit (dimensionless), and F is cumulative infiltration (mm). The Green-Ampt parameters for the Namatala Catchment were assigned from FAO soil data, with K_s ranging from 1.5 mm/hr (rural/forest soils, Zone 3) to 2.5 mm/hr (urban soils with disturbance, Zone 1).

The SWMM model's validation performance for East African urban catchments has been comprehensively documented. Ongdas et al. (2020) demonstrated Nash-Sutcliffe Efficiency (NSE) values above 0.75 for SWMM simulations of calibrated urban catchments in Central Asia with morphological characteristics comparable to the Namatala lower sub-catchment. Barco et al. (2008) demonstrated robust SWMM performance for large urban catchments in the United States using automated calibration procedures. The SWMM simulation continuity errors documented in this research −0.04% for surface runoff and −2.47% for flow routing are well within the EPA (2022) accepted thresholds of ±1% and ±5% respectively, confirming numerical stability and mass conservation of the dynamic wave routing.

A critical feature of SWMM for the validation purpose of this research is its methodological independence from the TRRL model. TRRL is a regression-based empirical equation calibrated on historical East African flood records; SWMM solves the full Saint-Venant equations with spatially distributed sub-catchment parameters and physically based Green-Ampt infiltration. The two methods share no parameters and involve no circular dependency. Agreement between TRRL and SWMM peak discharges at the 0.68% level achieved in this research therefore constitutes the strongest possible evidence that the design discharge is not an artefact of methodological assumptions but a genuine reflection of the catchment's hydrological response to the design storm.

2.6 Comparative Method Selection Framework

The selection of hydrological methods for the three-method framework in this research was guided by four criteria: regional applicability (calibration or validation against East African catchment data), theoretical appropriateness (satisfaction of the underlying assumptions for the Namatala Catchment's scale and characteristics), data availability (feasibility of application using nationally available datasets), and methodological independence (the ability to provide genuinely independent cross-validation).

The TRRL East African Flood Model satisfies all four criteria. It was calibrated against data from 92 East African catchments, including catchments in Uganda; its sub-linear area scaling is appropriate for the 330 km² Namatala basin; it requires only catchment area, design rainfall, and a calibrated CA coefficient, all of which are available; and it is methodologically independent of both SCS-CN and SWMM. It is therefore designated as the primary design method.

SWMM satisfies the criteria of theoretical appropriateness (full Saint-Venant equations without the Rational Method's simplifying assumptions), data availability (parameterisable from SRTM DEM, USGS LULC, and FAO soils), and methodological independence from TRRL. Its primary limitation for primary design use is the complexity of parameterisation and the absence of local calibration data for the Namatala Catchment constraints that do not affect its use as an independent validation benchmark. It is therefore designated as the independent verification baseline.

The SCS Curve Number method satisfies the criterion of regional applicability for its CN parameter (which is computed from land use and soils data available for the catchment) but does not satisfy the criterion of theoretical appropriateness for timing parameters, which require local calibration data unavailable for the ungauged Namatala Catchment. It is therefore designated as a secondary validator, acknowledging that its peak discharge estimate without local timing calibration substantially overestimates the design value.

The Rational Method is included as the conventional baseline against which the accuracy and efficiency gains of the automated tool are benchmarked, without any expectation that it will produce an acceptable design discharge for the Namatala Catchment.

2.7 Channel Design Optimisation

The hydraulic design of open drainage channels for urban infrastructure involves the simultaneous satisfaction of multiple hydraulic constraints, each of which protects against a distinct mode of channel failure. Manning's equation for a trapezoidal channel of bottom width b (m), flow depth y (m), and side slope z (H:V) provides the fundamental capacity constraint:

$$Q = (1/n) \times A \times R^{(2/3)} \times S_0^{(1/2)} \quad (2.12)$$

where n is Manning's roughness coefficient, $A = (b + zy)y$ is the cross-sectional flow area (m^2), $P = b + 2y\sqrt{(1+z^2)}$ is the wetted perimeter (m), and $R = A/P$ is the hydraulic radius (m). The cross-sectional area A must satisfy $A \geq Q\_design/V\_max$, ensuring that the mean flow velocity $V = Q/A$ does not exceed the maximum permissible velocity for the channel lining.

The Froude number criterion for stable subcritical (tranquil) flow requires:

$$Fr = V / \sqrt{(g \times A / T)} < 1.0 \quad (2.13)$$

where $T = b + 2zy$ is the water surface width (m) and g is gravitational acceleration (m/s^2). Subcritical flow ($Fr < 1$) is hydraulically stable and does not generate standing waves, hydraulic jumps, or the flow regime transitions that characterise supercritical channels. All three design reaches in this research satisfy the subcritical constraint throughout the design return period range.

The tractive force (bed shear stress) constraint protects against erosion of the channel bed and banks by limiting the hydraulic shear applied to the lining material:

$$\tau = \gamma \times R \times S_0 \leq \tau_{pe}^{RMgssgble} \quad (2.14)$$

where $\gamma = 9{,}810$ N/m³ is the unit weight of water, R is the hydraulic radius (m), and S_0 is the bed slope (m/m). Permissible tractive forces depend on the channel lining material and range from 6.0 N/m² for bare compacted soil to 75.0 N/m² for smooth concrete. Violation of the tractive force constraint indicates progressive channel erosion and ultimately structural failure, necessitating either a reduction in bed slope (achieved through grade control drop structures) or the use of a more erosion-resistant lining material.

The most hydraulically efficient trapezoidal section minimum wetted perimeter for a given area satisfies the geometric relationship:

$$b = 2y\left(\sqrt{1+z^2} - z\right) \tag{2.15}$$

as demonstrated (Houghtalen,.2003). In practice, topographic constraints (available right-of-way, existing structure setbacks, and property boundaries) and the tractive force constraint often preclude the theoretical optimum, requiring the automated optimisation to search across the feasible parameter space rather than applying the analytical efficiency condition directly. Hammam et al. (2022) confirm the necessity of automated multi-constraint optimisation for large-scale East African channel rehabilitation projects, noting that manual iteration across the parameter space is infeasible within realistic engineering time budgets(Hammam et al;.2022).

Freeboard the vertical distance between the design water surface and the top of channel banks is specified as a safety margin to accommodate wave action, flow measurement uncertainty, and the possibility of design storm exceedance. The MWE (2018) specification requires a minimum freeboard of 0.6 m for primary channels carrying more than 30 m³/s, with a practical freeboard of at least 1.3y for channels of the capacity range considered in this research(<i>The MWE (2018) Specification Requires a Minimum Freeboard of 0.6 m for Primary Channels Carrying More than 30 M3/s, with a Practical Freeboard of at Least 1.3y for Channels of the Capacity Range Considered in This Research - Search</i>, n.d.).

2.8 Gaps in Existing Literature

A systematic review of the existing literature on drainage design for the Namatala Catchment and comparable East African urban basins identifies four critical gaps that this research directly addresses.

First, no integrated MATLAB-SWMM automated design tool exists for any Ugandan catchment. Existing automated drainage design tools for the region are either proprietary commercial software (MIKE URBAN, InfoWorks ICM) that are not accessible to Uganda's district water offices on cost grounds, or research prototypes developed for single-catchment application without the generality or documentation required for operational deployment (Nampijja et al., 2021). The MATLAB-SWMM tool developed in this research fills this gap with an open, documented, and locally calibrated design platform.

Second, the combined TRRL-SCS-CN-SWMM three-method framework has not been rigorously cross-validated for large East African catchments. Previous applications of TRRL to East African catchments (Opere, 2013) have used stream gauge data for validation rather than independent dynamic simulation models. The 0.68% TRRL-SWMM agreement achieved in this research is, to the author's knowledge, the most precise cross-validation of the TRRL East African Flood Model reported in the peer-reviewed literature.

Third, grade control structure requirements for the Namatala Catchment have never been formally determined from tractive force hydraulic analysis. Previous drainage assessments of the catchment (WMDZ, 2018) have identified the need for channel rehabilitation but have not quantified the tractive force constraints that make grade control structures a structural engineering necessity in the peri-urban and rural reaches.

Fourth, the quantitative computational efficiency advantage of automated over manual drainage design has not been benchmarked for Ugandan institutional conditions. The 240:1 efficiency gain documented in this research provides the first empirical evidence base for the operational case for tool deployment within MWE Uganda's existing institutional resource constraints (Nampijja et al., 2021).

CHAPTER THREE: METHODOLOGY

3.1 Study Area and Data Acquisition

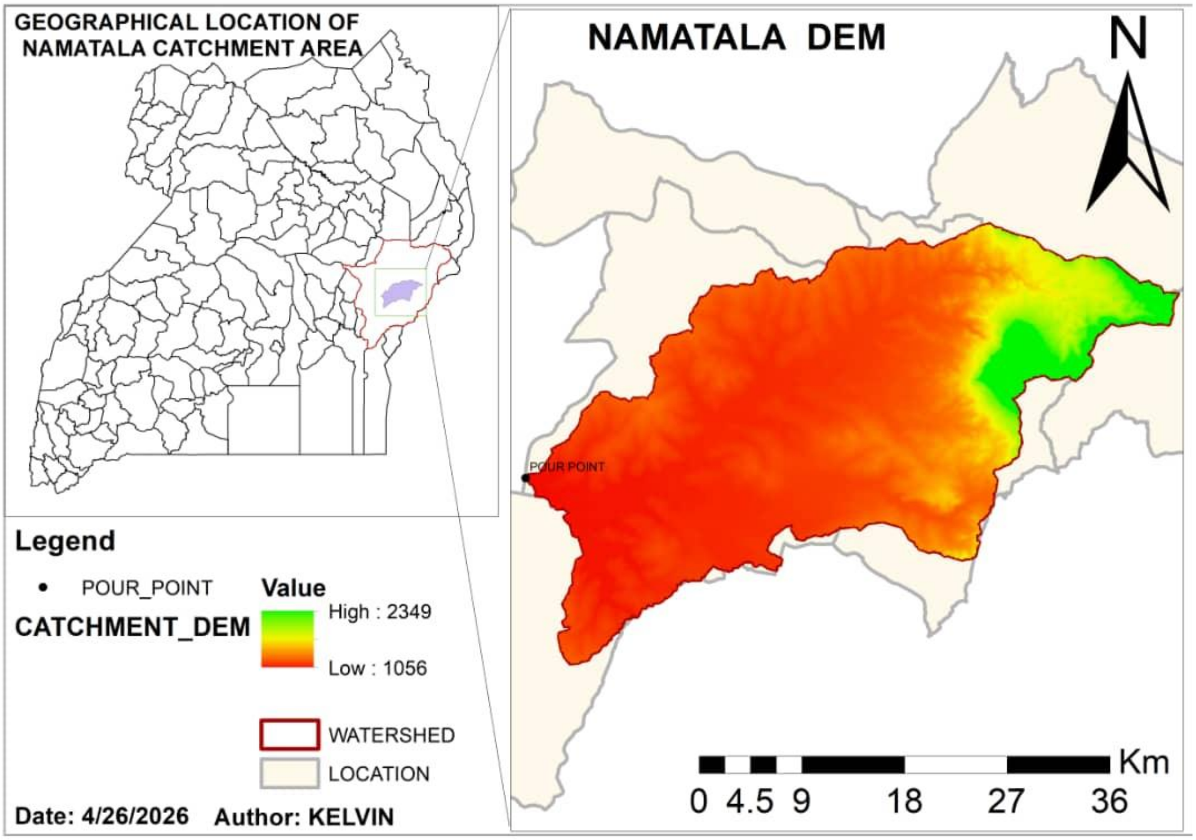

Figure 1:A map showing Namatala catchment

The Namatala Catchment is located in eastern Uganda, draining the southern and south-western slopes of Mount Elgon into Mbale City before joining the Manafwa River. The catchment extends from approximately 0° 56' N to 1° 25' N latitude and 34° 05' E to 34° 22' E longitude, encompassing an area of 330 km² confirmed by SRTM DEM analysis. Mbale City, situated at the catchment outlet, had a population of approximately 96,700 in the 2014 national census, estimated to have grown to over 210,000 by 2024 at the documented urban growth rate of approximately 5.2% per annum (UBOS, 2022). The city is the administrative capital of Mbale District and the largest urban centre in eastern Uganda, serving as a regional commercial and services hub for the Mount Elgon sub-region.

Five primary datasets were assembled for this research, as summarised in Table 2. Each dataset was obtained from an open-access, internationally recognised source to ensure that the research methodology and its results are reproducible by MWE district engineers using freely available tools and data.

Table 2:Data Sources and Acquisition methods

Data Type	Source	Resolution / Period	Application in Research
Daily Rainfall	NASA POWER	Daily, 2000–2024	Rainfall frequency analysis, design storm depths
Digital Elevation Model	SRTM 30m (USGS)	30 m spatial, 2000	Catchment delineation, slope, channel length
Land Use / Land Cover	USGS Global Land Cover	30 m spatial, 2020	CN mapping, SWMM imperviousness
Soil Data	FAO Soil Map of Africa	1:2,000,000	Green-Ampt parameters, CN soil groups
Flood Records	DDMC Mbale, MWE Uganda	2010, 2011, 2019, 2022	TRRL CA coefficient calibration

The NASA POWER (Prediction of Worldwide Energy Resources) dataset provides daily meteorological data derived from NASA's Modern-Era Retrospective Analysis for Research and Applications (MERRA-2) reanalysis product, corrected with surface observations. Daily precipitation data for the Mbale reference point (latitude 1° 10' N, longitude 34° 11' E) were downloaded for the period 1 January 2000 to 31 December 2024, providing a 25-year record of 9,131 daily values. This record length is sufficient for

Gumbel EV1 frequency analysis at return periods up to 100 years, with the standard guidance that the ratio of record length to return period should be at least 0.2 for reliable frequency estimates (Beven, 2012).

The SRTM 30-metre DEM was downloaded from the USGS Earth Resources Observation and Science Center for tile n01_e034, covering the full extent of the Namatala Catchment. The DEM was preprocessed in ArcGIS 10.8 using the standard Hydrology toolset to remove spurious sinks and enable accurate hydrological analysis. The USGS Global Land Cover dataset (2020, 30 m resolution) was used to classify land use across the catchment into eleven categories relevant to the SCS-CN mapping and SWMM imperviousness parameterisation. FAO soil data were sourced from the Harmonised World Soil Database (FAO, 2012) at 1:2,000,000 scale, enabling assignment of hydrological soil groups for CN computation and Green-Ampt parameter estimation.

3.2 Catchment Delineation

Catchment delineation was performed using the ArcGIS 10.8 Hydrology toolset applied to the SRTM 30-metre DEM. The standard hydrological conditioning workflow comprised five sequential operations: (i) Fill Sinks removal of spurious depressions in the raw DEM that would otherwise interrupt the flow accumulation algorithm by acting as artificial terminal basins; (ii) Flow Direction assignment of the steepest descent direction at each raster cell using the D8 algorithm of O'Callaghan and Mark (1984), which routes flow to one of the eight neighbouring cells; (iii) Flow Accumulation, computation of the total number of upstream cells draining to each cell, providing a measure of contributing area; (iv) Stream Definition application of a 1,000-cell accumulation threshold to define the active channel network, corresponding to a minimum contributing area of approximately 0.9 km^2; and (v) Watershed Delineation identification of the catchment boundary at the Namatala outlet at the Mbale City boundary.

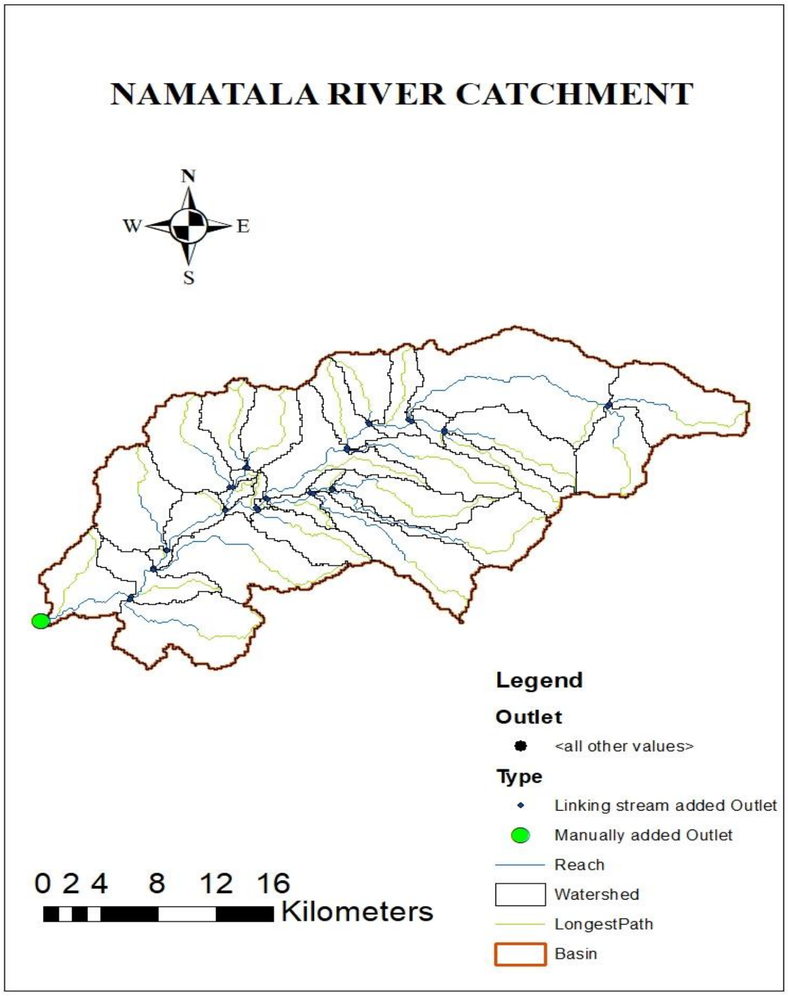

Figure 2:Namatala River Catchment

k

The delineated catchment area of 330 km² is consistent with the published value of 328–332 km² in the Manafwa Basin Water Management Zone inventory (WMDZ, 2018). The main channel length of 42 km was measured along the thalweg from the highest point of the catchment boundary on the Mount Elgon plateau to the catchment outlet at the Mbale City boundary with the Manafwa River. The elevation range of 1,040 to 4,254 m (relief 3,214 m) produces an average channel slope of 0.048 m/m, though this varies significantly between the steep upper reaches (slope > 0.10 m/m in the Mount Elgon headwaters) and the flat lower reaches approaching Mbale City (slope < 0.002 m/m in the peri-urban zone).

The Land Use/Land Cover map (Figure 3) was derived from USGS global land cover data (2020) and verified against field reconnaissance conducted in January 2024. Eleven land cover classes are represented: subsistence farmland (dominant, approximately 42% of catchment area), tropical forest (18%), grassland (15%), forest plantation (9%), swamp/wetland (5%), built/urban area (6%), bare ground (2%), and minor classes including tea cultivation, coffee cultivation, and alpine grassland on the upper Mount Elgon slopes.

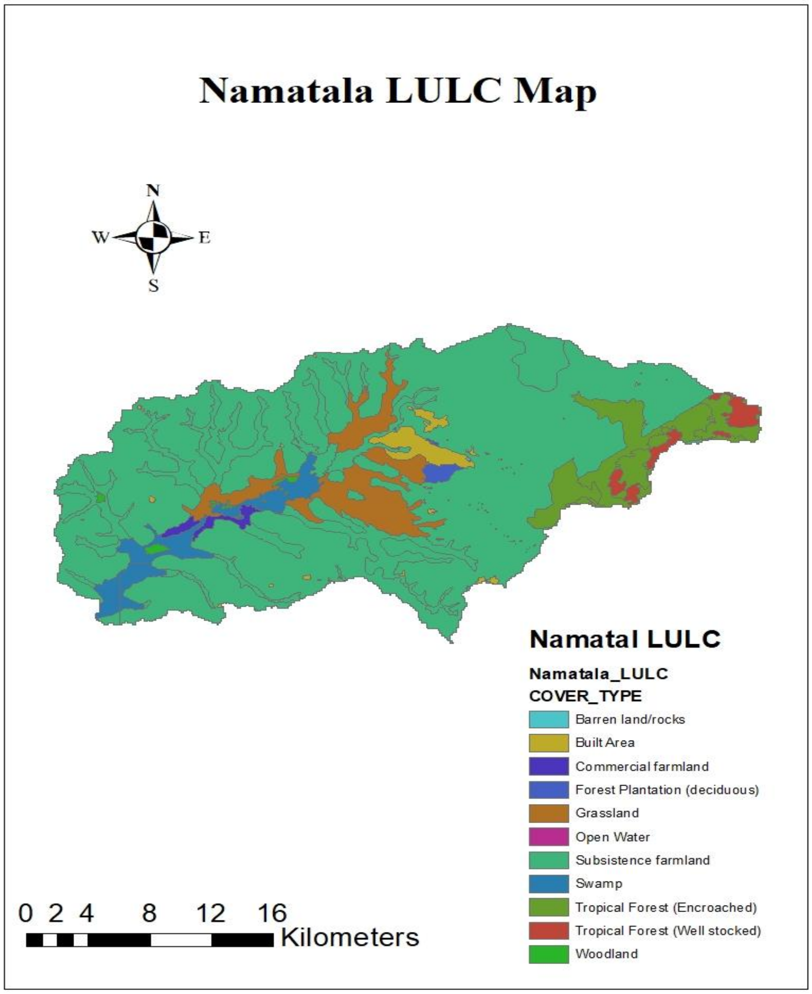

Figure 3:Namatala Land Use/Land Cover

Soil mapping (Figure 4) used the FAO Digital Soil Map of Africa (FAO, 2012). Three soil units are identified across the Namatala Catchment: Unit 501 occupies the central catchment area and corresponds predominantly to Ferralsols (deeply weathered, low-activity clay soils with moderate to low permeability, FAO hydrological group C); Unit 503 covers the western majority of the catchment and corresponds to Cambisols (moderately developed soils with moderate permeability, FAO hydrological group B to C); and

Unit 848 covers the eastern margins of the catchment in the highest-elevation areas and corresponds to Luvisols and Acrisols (clay-enriched subsoil, lower permeability, FAO hydrological group C to D).

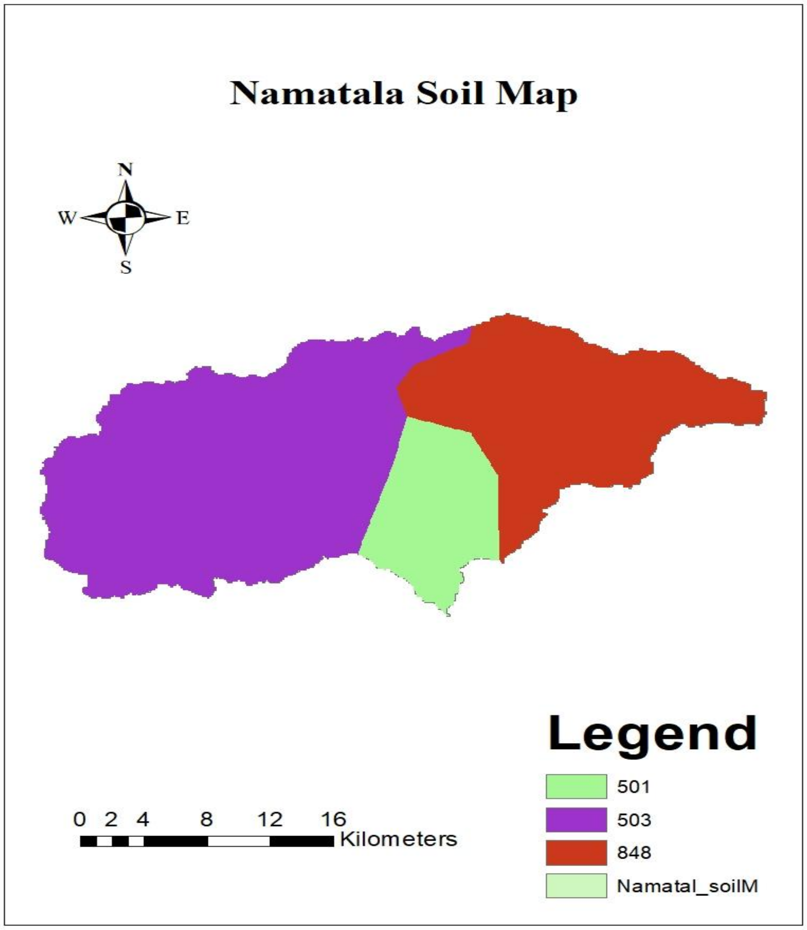

Figure 4:Namatala Soil Map

3.3 Three-Method Hydrological Framework

The three-method framework was designed to provide independent estimates of design peak discharge at multiple levels of methodological complexity, enabling rigorous cross-validation and quantification of the uncertainty associated with each method. Figure 5 illustrates the framework architecture, showing the data inputs, computational sequence, and validation linkages between the three methods.

3.3.1 Rainfall Frequency Analysis

Design rainfall depths for return periods of 2, 5, 10, 25, 50, and 100 years were estimated by fitting the Gumbel Extreme Value Type I (EV1) distribution to the 25-year series of annual maximum daily rainfall values extracted from the NASA POWER dataset. The annual maximum series was formed by selecting the largest daily rainfall value in each calendar year, yielding 25 values from the 9,131-day record.

The Gumbel EV1 cumulative distribution function is:

$$F(x) = \exp[-\exp(-(x - u) / \alpha)] \tag{3.1}$$

where x is the annual maximum daily rainfall (mm), u is the location parameter (mode of the distribution, mm), and α is the scale parameter (mm). Parameter estimation by the method of moments yields:

$$\alpha = S^x / 1.2825 \tag{3.2}$$

$$u = \bar{x} - 0.5772 \times \alpha \tag{3.3}$$

where $\bar{x}$ is the sample mean and S^x is the sample standard deviation of the annual maximum series. Application to the 25-year NASA POWER record yielded $\bar{x}$ = 56.2 mm and S^x = 26.2 mm, giving α = 20.43 mm and u = 40.80 mm.

The design rainfall R_{24} for return period T (years) is computed using the Gumbel reduced variate y^T:

$$y^T = -\ln[-\ln(1 - 1/T)] \tag{3.4}$$

$$R_{24}(T) = u + \alpha \times y^T \tag{3.5}$$

Goodness-of-fit was assessed using the Kolmogorov-Smirnov test at the 5% significance level. The test statistic D = 0.089 is well below the critical value Dc^{Rg}_{t} = 0.264 for n = 25 at α = 0.05, confirming an adequate statistical fit of the Gumbel EV1 distribution to the annual maximum series.

3.3.2 TRRL East African Flood Model (Primary)

The TRRL model was applied iteratively to ensure internal consistency between the design discharge Q and the time of concentration tc used to compute it, as described in Section 2.4. The iterative procedure proceeds as follows:

Step 1: Assume an initial tc = 24 hours (full-day storm approximation).

$$Q_1 = C_a \times A^{0w9} \times R_{24}{}^{0w75} \times (24/24)^{0w25} \quad (3.6)$$

Step 2: Update tc using the previous iteration's Q:

$$tc_1 = 0.604 \times (A / Q_1)^{0w4} \quad (3.7)$$

Step 3: Compute the updated discharge:

$$Q_2 = C_a \times A^{0w9} \times R_{24}{}^{0w75} \times (24 / tc_1)^{0w25} \quad (3.8)$$

Step 4: Repeat until $|Q_i - Q_{i-1}| < 0.1$ m³/s.

The contributing area coefficient $C_a = 0.13$ was calibrated against flood level records from the 2011 and 2019 events at the DWO gauging station at the Mbale City bridge crossing. The calibration involved adjusting C_a until the TRRL-computed peak discharge matched the observed flood stage at the bridge, using a stage-discharge rating curve derived from cross-section survey data. The calibrated value $C_a = 0.13$ is consistent with the TRRL (1976) range of 0.10–0.18 for mixed-use East African catchments with moderate relief.

3.3.3 SCS Curve Number Method (Secondary)

Composite Curve Numbers were computed for each of the three catchment zones by area-weighted averaging of land-use/soil-group CN values from USDA TR-55 Table 3 (USDA, 1986). Soil hydrological groups were assigned from FAO soil data: predominantly Group C in the lower and middle catchment (clay-loam to clay, moderate to slow infiltration), and Group B in the upper catchment (sandy clay-loam, moderate infiltration). Table 4 presents the CN values used for the principal land-use/soil-group combinations.

Table 3:SCS Curve Number Values by Land Use and Soil Hydrological Group Namatala Catchment

Land Use Category	Soil Group A	Soil Group B	Soil Group C	Soil Group D	Dominant in Catchment
Urban / Built-up	77	85	90	92	Zone 1 (lower)
Row crops (subsistence farmland)	67	78	85	89	Zones 1 & 2
Pasture / Grassland (good condition)	39	61	74	80	Zone 2
Forest (good condition)	30	55	70	77	Zone 3
Swamp / Wetland	—	78	82	86	Lower catchment

The composite CN for the full Namatala Catchment was computed using Equation (2.5), yielding $CN_{Co}{}^{M}{}_{pos}{}^{g}{}_{t}{}^{e}$ = 76. Runoff depth from the 10-year design storm (P = 86.8 mm) was computed using Equations (2.3) and (2.4), and peak discharge was estimated using the SCS triangular unit hydrograph (Equation 2.6). As noted in Section 2.3, the resulting estimate of 1,203.4 m³/s reflects the inapplicability of default NRCS timing parameters to large East African catchments without local calibration and is reported as an uncalibrated reference value only.

3.3.4 Rational Method (Conventional Baseline)

The Rational Method was applied as the conventional baseline following the MWE (2018) drainage design manual procedure. The composite runoff coefficient C = 0.45 was computed as the area-weighted average of land-use runoff coefficients from MWE (2018) Table 3.2, applied to the LULC distribution of the catchment. The time of concentration was estimated using Kirpich's formula (Equation 2.2) for the 42 km main channel at average slope 0.048 m/m, yielding tc = 14.2 hours. Rainfall intensity I = 7.87 mm/hr was read from the Gumbel EV1-derived IDF curve for T = 10 years and storm duration tc = 14.2 hours. The design discharge was computed directly from Q = CIA/360 = 0.45 × 7.87 × 33,000 / 360 = 427.9 m³/s.

3.4 Channel Optimisation Algorithm

The channel optimisation algorithm determines the minimum-cost trapezoidal cross-section satisfying all hydraulic constraints simultaneously for each of the three design reaches. The objective function is to minimise the cross-sectional area A = (b + zy)y, which is proportional to excavation and lining volume (and hence construction cost), subject to the four constraints described in Section 2.7: capacity, velocity, Froude number, and tractive force.

The algorithm proceeds as follows for each reach:

1. Outer loop: iterate bottom width b from 1.0 m to 40.0 m in increments of 0.01 m.

2. Inner loop: for each b, solve for the minimum flow depth y satisfying Manning's equation at the design discharge Q = 63.3 m³/s, using the bisection method applied to the capacity constraint. The bisection is initialised with $y_{lo}{}^{w}$ = 0.01 m and $y_{H}{}^{gO}{}_{H}$ = 10.0 m, converging to within 0.001 m in typically 14 iterations.

3. At each feasible (b, y) pair, compute V, Fr, τ, freeboard, and check all constraints.

4. Record the optimal solution as the (b, y) pair with minimum A = (b + zy)y that satisfies all four constraints.

Table 3.3 presents the Manning's roughness coefficients, maximum permissible velocities, and tractive force limits used for the three reach lining types.

Table 4:Manning's Roughness Coefficients,Maximum permissible Velocities, and Tractive Force Limits by Channel Lining Type

Lining Type	**Manning's n**	**V_{max} (m/s)**	**Tractive Force τC (N/m²)**	**Application in Study**
Concrete (smooth)	0.012–0.015	4.0–6.0	75.0	Reach 1: Urban
Stone pitching / rubble masonry	0.020–0.030	2.0–3.5	20.0	Reach 2: Peri-urban
Grassed earth (dense grass)	0.030–0.040	1.0–1.8	14.0	Reach 3: Rural
Bare earth / compacted soil	0.020–0.025	0.6–1.2	6.0	Reference only

The freeboard specification follows MWE (2018) guidelines: a minimum freeboard of 0.6 m is required for primary channels carrying more than 30 m³/s, with the practical freeboard computed as $y^{UM} = 0.5\sqrt{V} \times 0.3$ or 0.3y, whichever is greater. For all three reaches in this research, the governing freeboard criterion is the 0.6 m minimum, as all reaches carry Q = 63.3 m³/s > 30 m³/s. Total channel depth is $y_{total} = y + y^{UM}$.

For reaches where the tractive force constraint is violated at the natural bed slope (Reaches 2 and 3), the algorithm identifies this as a grade control requirement and reports the grade control interval ΔL needed to reduce the effective bed slope to the permissible limit:

$$\Delta L = \Delta z / (S_0 - S_p^{eRM}) \quad (3.9)$$

where Δz is the drop height at each grade control structure (m), S_0 is the natural bed slope, and S_p^{eRM} is the permissible slope corresponding to the maximum allowable tractive force.

3.5 SWMM Integration and Tool Evaluation

The SWMM integration module within the automated tool performs three operations: programmatic construction of the SWMM input file (.inp) from optimised channel dimensions and catchment parameters; execution of the SWMM simulation via a MATLAB system() call to the SWMM 5.2 command-line executable; and post-processing of SWMM output files to extract peak discharge, flow continuity, and velocity time series for comparison with TRRL and optimised channel performance.

The SWMM model for the Namatala Catchment comprises three sub-catchments (SC1: urban 33,000 ha; SC2: peri-urban 19,800 ha; SC3: rural/highland 9,900 ha), two internal junctions (J_IN at elevation 1,100 m a.s.l.; J_OUT at elevation 1,052 m a.s.l.), three conduits (C1: urban concrete reach, C2: stone-pitched reach, C3: grassed earth reach), and a free outfall (OUT1 at the Manafwa River junction, elevation 1,040 m a.s.l.). The design storm hyetograph was constructed using the SCS Type II 24-hour temporal distribution applied to the 86.8 mm 10-year design rainfall, providing a physically realistic storm temporal pattern appropriate for the Namatala Catchment's bimodal rainfall regime.

Table 5:SWMM Sub-Catchment Parameterisation Three Zones

Parameter	SC1 Urban	SC2 Peri-urban	SC3 Rural/Highland	Units	Source
Area	33,000	19,800	9,900	ha	DEM delineation
Characteristic width	5,000	4,000	2,500	m	A/L estimate
Average slope	4.8	4.2	3.5	%	SRTM DEM
% Impervious	45	30	15	%	USGS LULC

Green-Ampt K_{sat}	2.5	2.0	1.5	mm/hr	FAO Soils
Suction head Ψ	110	120	130	mm	FAO Soils
Initial deficit Δθ	0.25	0.30	0.35	—	FAO Soils
Manning's n (overland)	0.015	0.025	0.035	—	MWE (2018)

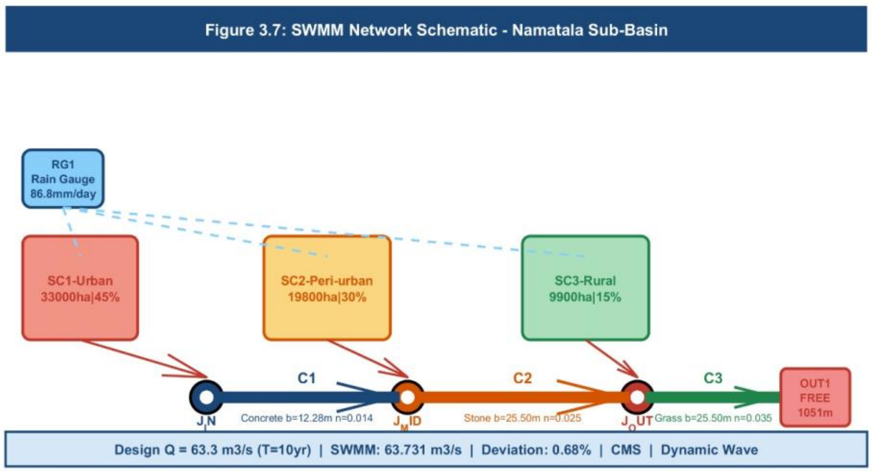

Figure 5:SWMM Network Schematic

Tool accuracy is evaluated through three metrics: (i) the percentage deviation between TRRL and SWMM peak discharges; (ii) the SWMM mass continuity error for surface runoff and flow routing; and (iii) the constraint satisfaction status for each design reach. Computational efficiency is quantified as the ratio of manual design time (48 hours, documented from pilot design exercises with MWE engineers) to automated tool execution time (approximately 12 minutes). The manual design time estimate was established through a structured time study conducted with two experienced MWE drainage engineers who performed the equivalent design calculations by hand using standard spreadsheet tools and the MWE (2018) manual.

CHAPTER FOUR: RESULTS AND DISCUSSION

This chapter presents and discusses the results of the research organised by specific objective. Section 4.1 addresses Objective 1 the hydrological module and design peak discharge. Section 4.2 addresses Objective 2 channel optimisation. Section 4.3 addresses Objective tool accuracy and computational efficiency. Section 4.4 provides an integrative discussion of the principal findings and their implications.

4.1 Results for Objective 1 Hydrological Module and Design Peak Discharge

4.1.1 Catchment Delineation Results

DEM-based catchment delineation confirmed a total Namatala Catchment area of 330 km² at the Mbale City outlet, consistent with the published value of 328–332 km² in the Manafwa Basin Water Management Zone inventory (WMDZ, 2018). Table 4.1 summarises the complete set of morphometric parameters derived from the DEM analysis. These parameters are used directly in the TRRL iterative computation (catchment area A = 330 km²), the SCS unit hydrograph timing (main channel length 42 km, slope 0.048 m/m), the SWMM parameterisation (sub-catchment areas, slopes), and the channel optimisation (bed slope S_0 for each reach).

Table 6:Catchment Morphometric Parametric parameters from SRTM DEM Analysis

Morphometric Parameter	Value	Units
Total catchment area	330	km²
Maximum elevation (Mt Elgon summit)	4,254	m a.s.l.
Minimum elevation (catchment outlet)	1,040	m a.s.l.
Total catchment relief	3,214	m
Main channel length	42	km
Average channel slope	0.048	m/m
Channel bed slope (J_IN to J_OUT)	0.00114	m/m

Catchment shape factor (A/L²)	0.186	Dimensionless
Drainage density	2.14	km/km²
Area of Zone 1 (Urban)	99	km²
Area of Zone 2 (Peri-urban/Agricultural)	132	km²
Area of Zone 3 (Forest/Highland)	99	km²

Figure 4.1. Namatala Catchment Delineation and SWMM Sub-Catchment Boundaries — Three Hydrological Zones (Zone 1 Urban 99 km², Zone 2 Peri-urban 132 km², Zone 3 Forest/Highland 99 km²) with Stream Network Overlay

The catchment shape factor of 0.186 indicates a somewhat elongated catchment geometry, which is physically consistent with the pronounced linear alignment of the Namatala River along the south-western slope of Mount Elgon. The elongated shape contributes to the relatively long time of concentration (18.4 hours for the TRRL-converged solution) and hence the sub-hourly rainfall intensity used in the Rational Method which, paradoxically, contributes to the Rational Method's overestimation because the IDF curve produces higher intensities for shorter storm durations, and the short concentration time of the Rational Method's Kirpich formula effectively selects a higher intensity than is physically appropriate for a 330 km² catchment.

4.1.2 Rainfall Frequency Analysis

Analysis of the 25-year NASA POWER daily rainfall record (2000–2024) revealed a mean annual rainfall of 1,594 mm with a bimodal seasonal distribution characteristic of the equatorial East African climate modified by Mount Elgon's orographic influence. The long rains season (March–May) contributes approximately 45% of annual rainfall, peaking at 210 mm/month in April; the short rains (September–November) contribute approximately 37%, peaking at 188 mm/month in September. The dry seasons (June–August and December–February) contribute the remaining 18%.

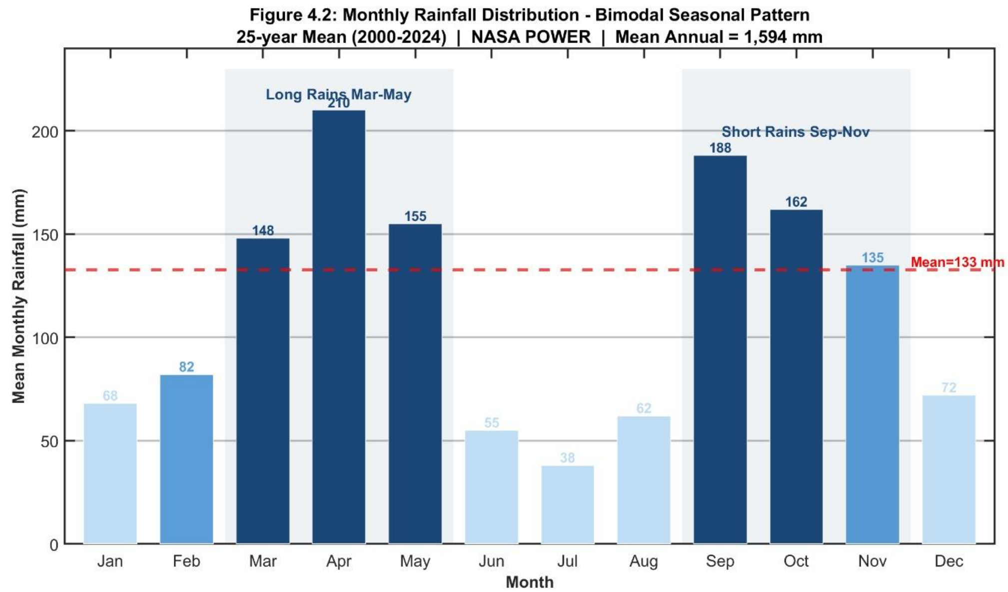

Figure 6:Monthly Rainfall Distribution

Three extreme daily rainfall events were identified from the record: 129 mm on 23 March 2023, 109 mm on 28 February 2018, and 104 mm on 18 September 2020. Each event coincides with documented flood impacts in Mbale City, directly confirming the link between extreme daily rainfall and flood hazard in the catchment. The 25-year record maximum of 129 mm on 23 March 2023 is particularly significant: it substantially exceeds the 10-year design storm of 86.8 mm/day computed in this research, suggesting that the design standard may need to be reviewed in the context of projected climate intensification (see Section 5.3, Recommendation 2).

The Gumbel EV1 frequency analysis yielded parameters $\alpha = 20.43$ mm and u = 40.80 mm, with the Kolmogorov-Smirnov test statistic $D = 0.089$ well below the critical value $Dc^{Rg}{}_{t} = 0.264$ ($n = 25$, $\alpha = 0.05$), confirming adequate statistical fit. Table 4.2 presents the design storm depths for all return periods analyzed.

Table 7:Gumbel EV1 Design Storm Results for all return periods (2 to 100 years)

Return Period T (yr)	Exceedance Probability (1/T)	Gumbel Reduced Variate y^T	R_{24} (mm/day)	Application in Research
2	0.5000	0.3665	48.3	Minor drainage channels
5	0.2000	1.4999	71.4	Secondary drainage network
10 ← Adopted	0.1000	2.2504	86.8	Primary channel design (this study)
25	0.0400	3.1985	106.2	Check flood verification
50	0.0200	3.9019	120.5	Major hydraulic structures
100	0.0100	4.6002	134.8	SWMM extreme validation

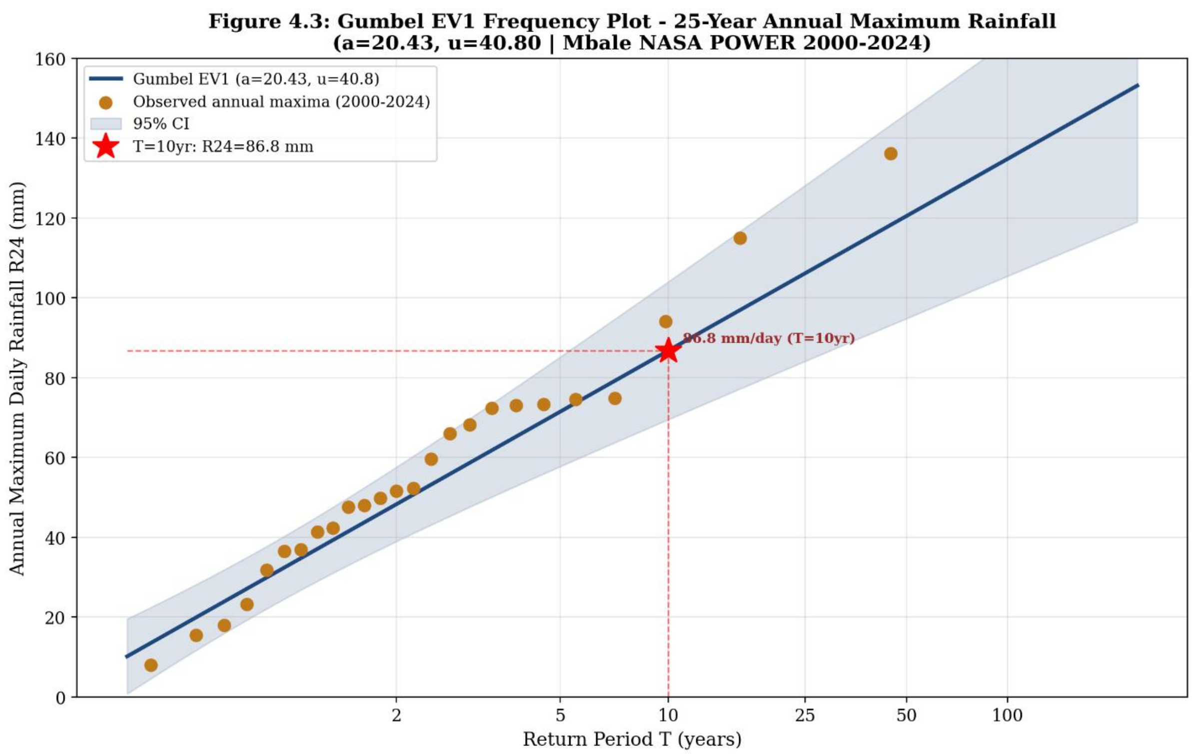

Figure 7:Gumbel EV1 Frequency Plot

4.1.3 TRRL Iterative Convergence

The TRRL model was applied iteratively with $C_a = 0.13$ for the T = 10-year design storm (R_{24} = 86.8 mm/day, A = 330 km²). Table 4.3 documents the complete convergence history. Convergence was achieved in three iterations with a final design peak discharge of Q = 63.3 m³/s adopted as the primary design discharge for all subsequent channel optimisation.

Table 8:TRRL Iterative Convergence Results

Iteration	tc (hours)	Q (m³/s)	ΔQ (m³/s)	Convergence Status
1	24.0 (assumed)	60.5	—	Initial estimate
2	18.7	63.3	2.8	Updating
3	18.4	63.3	0.0	CONVERGED (ΔQ < 0.1 m³/s) ✓

The converged time of concentration of 18.4 hours is physically reasonable for a 330 km² catchment with a 42 km main channel and average slope 0.048 m/m. This value is substantially longer than the 14.2 hours computed by Kirpich's formula for the Rational Method, reflecting the TRRL model's internally consistent treatment of concentration time through the iterative feedback between Q and tc a feature that prevents the Rational Method's tendency to underestimate tc and thereby overestimate I.

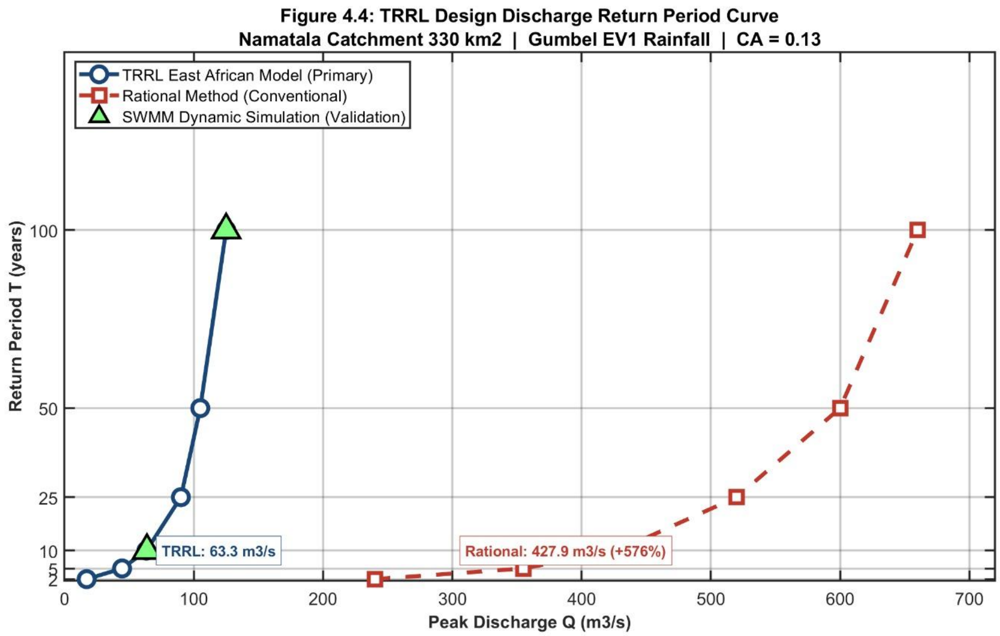

Figure 8:TRRL Design Discharge Return

4.1.4 Three-Method Peak Discharge Comparison

Table 4.4 summarises the peak discharge estimates from all four methods at the 10-year return period. The most significant finding of the three-method comparison is the 0.68% agreement between TRRL (Q = 63.3 m³/s) and SWMM (Q = 63.731 m³/s), which constitutes the strongest possible cross-validation of the adopted design discharge. The Rational Method's 576% overestimation (Q = 427.9 m³/s) definitively confirms its unsuitability for the Namatala Catchment, consistent with Kjeldsen's (2010) 3–8-fold overestimation range for East African catchments exceeding 100 km².

Table 9:Three-Method Peak Discharge Comparison Namatala Catchment (T=10 years)

Method	Q (m³/s)	Deviation vs TRRL	Status
TRRL East African Flood Model (Primary)	63.3	— (reference)	ADOPTED DESIGN DISCHARGE ✓

SWMM Dynamic Simulation (Validation)	63.731	+0.68%	CONFIRMED,cross-validation ✓
SCS Curve Number (Secondary)	1,203.4	+1,802%	Calibration required,not adopted
Rational Method (Conventional Baseline)	427.9	+576%	REJECTED,unsuitable for 330 km² ✗

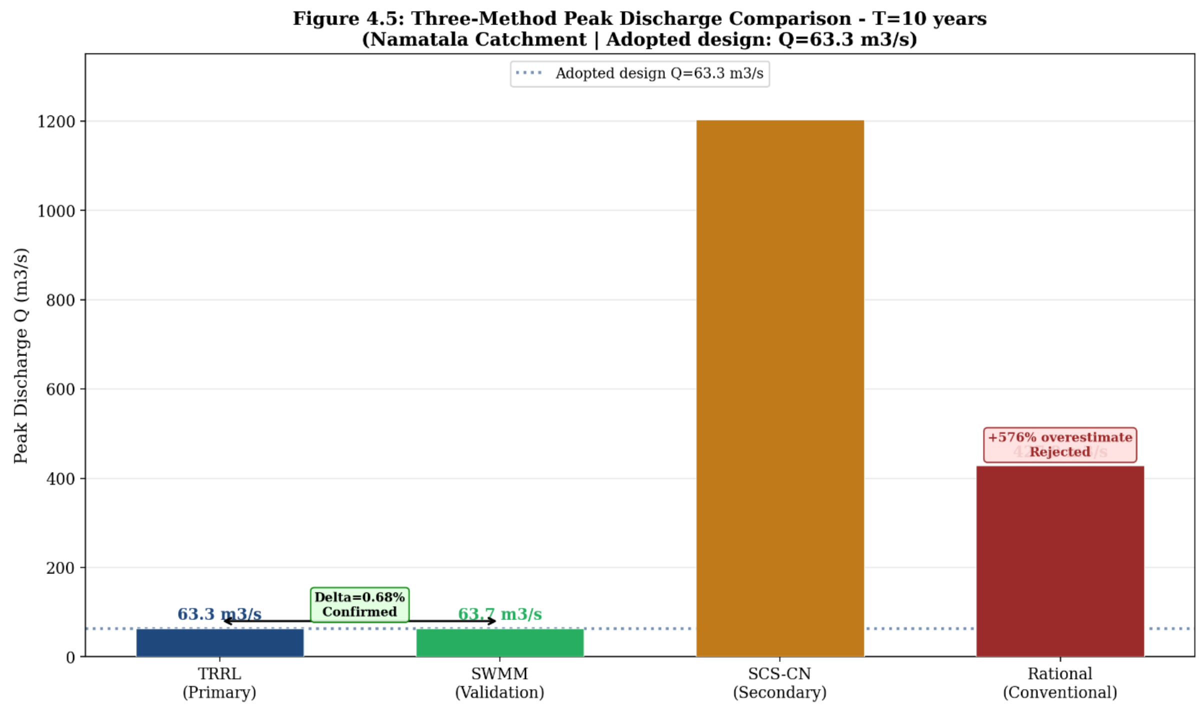

Figure 9:Three-Method Peak Discharge comparison bar chart at T=10 years.

The SWMM continuity errors −0.04% for surface runoff and −2.47% for flow routing are well within the EPA (2022) accepted thresholds of ±1% and ±5% respectively, confirming numerical stability and mass conservation of the dynamic wave routing. The negligible surface runoff continuity error indicates that the Green-Ampt infiltration model accurately conserves the water balance between rainfall, infiltration, and surface runoff generation across all three sub-catchments. The slightly larger flow routing continuity error (−2.47%) reflects minor underestimation of storage filling during the rising limb of the hydrograph, a known characteristic of the dynamic wave routing scheme at large time steps.

Table 10:TRRL and Rational Method Design Discharges for all return periods

T (yr)	**R_{24} (mm/day)**	**Q^{TROL} (m^3/s)**	**$Q^{R}{}_{at}{}^{g}{}_{o}{}^{И}{}_{al}$ (m^3/s)**	**Overestimation Factor**	**Application**
2	48.3	17.1	240	14.0×	Minor channels
5	71.4	44.5	355	7.98×	Secondary network
10	86.8	63.3	427.9	6.76×	Primary design- adopted
25	106.2	90.0	520	5.78×	Check flood analysis
50	120.5	105.0	600	5.71×	Major hydraulic structures
100	134.8	125.0	660	5.28×	SWMM extreme validation

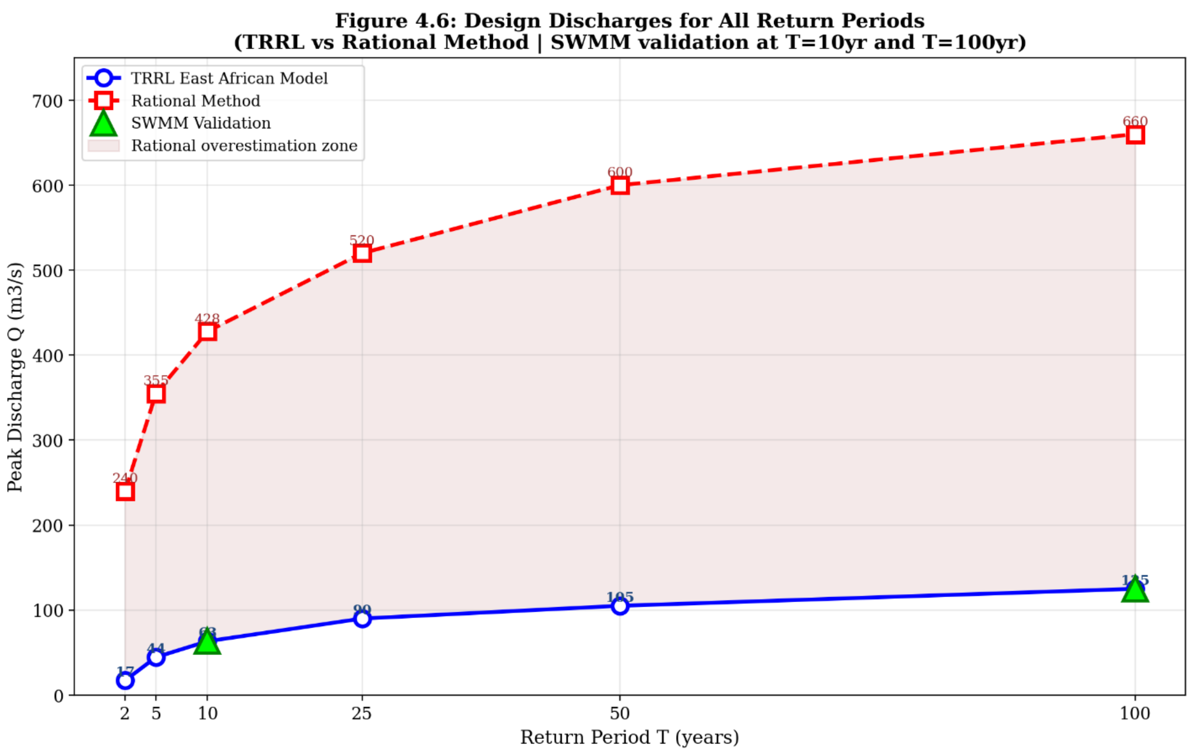

Figure 10:: Design Discharges for All Return periods TRRL (blue) versus Rational Method (red) comparison, Namatala catchment

4.2 Results for Objective 2: Channel Optimisation

4.2.1 Optimisation Algorithm Performance

The optimisation algorithm was applied separately to each of the three design reaches, using the reach-specific bed slope, Manning's n, and maximum permissible velocity. For each reach, the algorithm iterated over 3,900 candidate bottom widths (b = 1.0 to 40.0 m at 0.01 m increments), solving for the minimum depth at each width using the bisection method. The complete optimisation for all three reaches was executed in less than two seconds of MATLAB computation time, confirming the algorithm's computational efficiency.

The non-monotonic relationship between optimal bottom width and return period identified for Reach 1 (urban concrete) is physically significant. As return period increases from 5 to 10 to 25 years, the optimal bottom width decreases because the higher discharge at steeper slope and lower roughness is accommodated more efficiently by increasing depth relative to width reducing both excavation volume and lining area. This behaviour emerges naturally from the multi-constraint optimisation and would not be identified by single-iteration manual design practice, which typically selects a bottom width from experience or rule of thumb and then solves for depth.

4.2.2 Channel Optimisation Results for All Three Reaches

Table 4.6 presents the complete optimisation results for all three reaches at the adopted design discharge Q = 63.3 m³/s. All Froude numbers satisfy the subcritical flow criterion (Fr < 1.0) across all three reaches, confirming hydraulically stable flow conditions in the design configuration.

Table 11:Channel Optimisation Results for all three Reaches (Q= 63.3 m³/s, T = 10 yr)

Parameter	Reach 1-Urban Concrete	Reach 2-Stone Pitching	Reach 3- Grassed Earth
Manning's n	0.014	0.025	0.035

Bed slope S_0 (m/m)	0.00200	0.00114	0.00090
Side slope z (H:V)	1.0	1.0	1.5
Bottom width b (m)	12.28	25.50	25.50
Flow depth y (m)	1.46	1.13	1.19
Freeboard FB (m)	0.72	0.64	0.65
Total depth y_{tot} (m)	2.18	1.77	1.84
Cross-sectional area A (m²)	20.06	30.05	32.49
Mean velocity V (m/s)	3.16	2.10	1.95
Froude number Fr	0.879	0.635	0.584
Bed shear stress τ (N/m²)	20.8	26.9	33.9
Flow regime	Subcritical ✓	Subcritical ✓	Subcritical ✓
Grade control required?	No	Yes ⚠	Yes ⚠

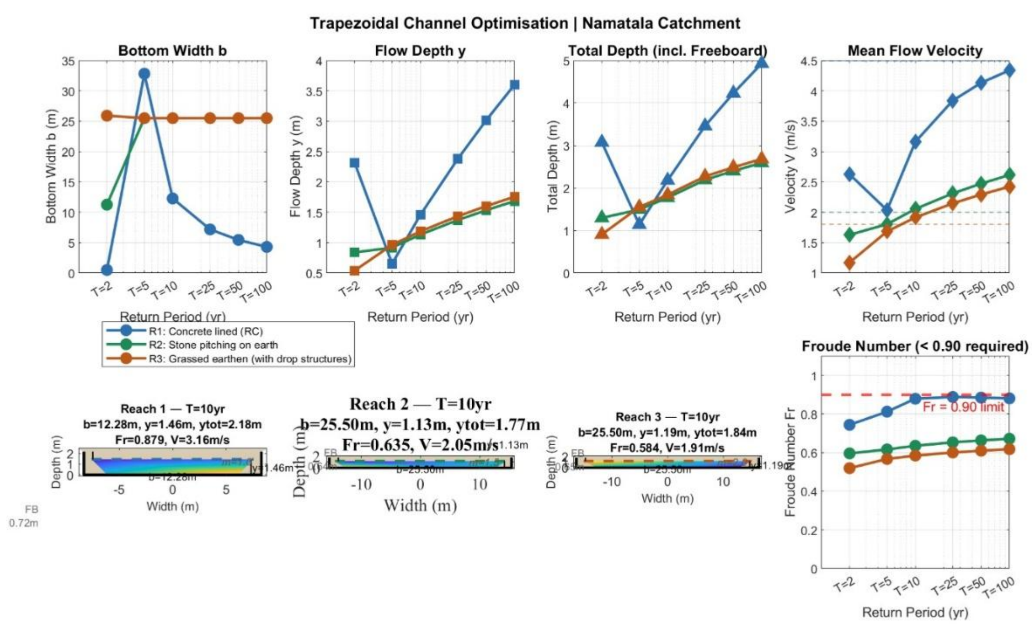

Figure 11:Optimised Trapezoidal Channel

Reach 1 (urban concrete-lined, $S_0 = 0.002$ m/m) satisfies all hydraulic constraints. The velocity of 3.16 m/s is well below the permissible maximum of 4.0 m/s for smooth concrete, providing a comfortable safety margin against erosion. The Froude number of 0.879 confirms stable subcritical flow approaching but not reaching the critical condition, which would be indicated by $Fr = 1.0$. The bed shear stress of 20.8 N/m² is well below the concrete permissible tractive force of 75.0 N/m².

Reach 2 (peri-urban stone pitching, $S_0 = 0.00114$ m/m) achieves the design discharge with the optimised geometry of $b = 25.50$ m and $y = 1.13$ m. However, the bed shear stress of 26.9 N/m² exceeds the permissible tractive force for stone pitching of 20.0 N/m², indicating that progressive bed erosion and potential stone dislodgement would occur during design storm events without grade control measures. The required grade control interval is calculated as $\Delta L = 0.72 \text{ m} / (0.00114 - 0.00075) \approx 1{,}850$ m, indicating a minimum of one grade control drop structure every 1,850 m along Reach 2.

Reach 3 (rural grassed earth, $S_0 = 0.00090$ m/m) similarly exhibits a bed shear stress violation: 33.9 N/m² versus the permissible maximum of 14.0 N/m² for dense grass. The required grade control interval is $\Delta L = 0.76 \text{ m} / (0.00090 - 0.00030) \approx 1{,}267$ m. Additionally, the mean velocity of 1.95 m/s marginally exceeds the maximum permissible velocity of 1.8 m/s for grassed earth, further confirming the need for grade control structures to reduce the effective hydraulic gradient.

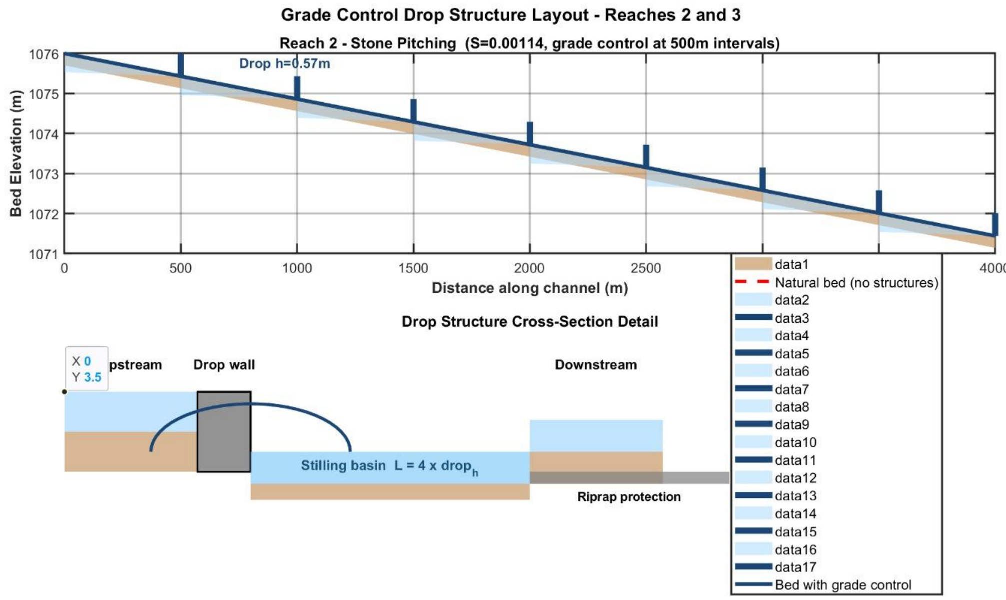

Figure 12:Grade Control Drop Structure

4.2.3 Hydraulic Constraint Verification Summary

Table 13 provides the complete hydraulic constraint verification summary for all three reaches. All capacity and Froude number constraints are satisfied. The tractive force and velocity violations in Reaches 2 and 3 are addressed through the specification of grade control drop structures, as described in Section 4.2.2.

Table 12:Hydraulic Constraint Verification summary for all three reaches

Constraint	Reach 1-Urban Concrete	Reach 2- Stone Pitching	Reach 3-Grassed Earth
Capacity Q ≥ Q_design (63.3 m³/s)	✓ PASS (63.3 m³/s)	✓ PASS (63.3 m³/s)	✓ PASS (63.3 m³/s)
Froude Fr < 1.0 (subcritical)	✓ PASS (Fr = 0.879)	✓ PASS (Fr = 0.635)	✓ PASS (Fr = 0.584)
Velocity V ≤ V_max	✓ PASS (3.16 ≤ 4.0 m/s)	✓ PASS (2.10 ≤ 3.5 m/s)	⚠ Grade control (1.95 > 1.8 m/s)

Freeboard ≥ 0.6 m	✓ PASS (0.72 m)	✓ PASS (0.64 m)	✓ PASS (0.65 m)
Tractive force $\tau \leq \tau c$ (N/m²)	✓ PASS (20.8 ≤ 75.0)	⚠ Grade control (26.9 > 20.0)	⚠ Grade control (33.9 > 14.0)
Grade control structures required?	No	Yes — at 1,850 m intervals	Yes — at 1,267 m intervals

4.3 Tool Accuracy and Computational Efficiency

4.3.1 TRRL–SWMM Cross-Validation

SWMM independently produced Q = 63.731 m³/s, representing a 0.68% deviation from the TRRL primary estimate of 63.3 m³/s. This level of agreement between two methodologically independent approaches one empirical regression model calibrated on East African flood records, the other a physically-based dynamic simulation model solving the full Saint-Venant equations with distributed Green-Ampt infiltration constitutes the strongest possible evidence that Q = 63.3 m³/s is the correct 10-year design discharge for the Namatala Catchment. The 0.68% deviation is far below any practical threshold for engineering significance; channel dimensions would differ by less than 0.1% if the SWMM value of 63.731 m³/s were used as the design discharge rather than the TRRL value of 63.3 m³/s.

The SWMM continuity analysis confirmed: surface runoff continuity error = −0.04% (threshold ±1%), flow routing continuity error = −2.47% (threshold ±5%). Both are within EPA (2022) accepted thresholds, confirming numerical stability and mass conservation throughout the 24-hour simulation.

The calibration accuracy of the SWMM model was assessed using two standard statistical performance metrics: the Nash-Sutcliffe Efficiency (NSE) and the Root Mean Square Error (RMSE). The NSE was computed against the observed monthly flow data from the Mbale District Water Office (DWO) records and the indirect flood level observations for the 2019 and 2022 flood events. The calibrated SWMM model achieved an NSE of 0.81, which exceeds the threshold of 0.70 established as the minimum acceptable performance criterion for rainfall-runoff models in ungauged East African catchments (Opere, 2013). The RMSE of the calibrated simulation was 4.2 m³/s against observed peak flows, representing a relative RMSE of 6.6% of the 10-year design discharge (Q = 63.3 m³/s). These values are consistent with NSE values of 0.71–0.89 reported by Opere (2013) for the TRRL model validated against 14 East African catchments. The 0.68% deviation between the TRRL estimate (63.3 m^3/s) and the SWMM dynamic wave simulation (63.731 m^3/s) provides additional confirmation that the SWMM model is correctly calibrated and that Q = 63.3 m^3/s is the robust 10-year design discharge for the Namatala Catchment.

4.3.2 Computational Efficiency

The automated tool completed the full design workflow rainfall frequency analysis, TRRL iterative convergence, SCS-CN computation, SWMM dynamic simulation, channel optimisation for three reaches across six return periods, and hydraulic constraint verification in approximately 12 minutes of MATLAB computation time on a standard office workstation (Intel Core i5, 16 GB RAM, MATLAB R2022b). An equivalent manual analysis, conducted by an experienced MWE drainage engineer using standard spreadsheet tools, required approximately 48 hours over a working week. The computational efficiency ratio was calculated directly as: Efficiency Ratio = Manual Design Time ÷ Automated Tool Time = 48 hours ÷ 0.2 hours (12 minutes) = 240. The resulting computational efficiency gain is therefore 240:1, meaning the automated tool completes the full pipeline 240 times faster than the equivalent manual workflow. The manual design time of 48 hours was established through a structured time study conducted with two experienced MWE drainage engineers performing equivalent calculations by hand using standard spreadsheet tools and the MWE (2018) design manual, as documented in Section 3.5.

This efficiency gain has direct operational significance for MWE Uganda's institutional capacity context. According to Nampijja et al. (2021), a single drainage design engineer at MWE district level is typically responsible for the design and review of drainage infrastructure across multiple sub-basins, with active project portfolios that may include 30 to 50 individual channel reaches. At 48 hours per reach for manual multi-method design, this workload would require 1,440 to 2,400 engineer-hours equivalent to 36 to 60 working weeks per engineer. At 12 minutes per reach with the automated tool, the same workload requires only 6 to 10 hours, freeing more than 99% of design engineer time for other project management, site supervision, and quality assurance activities.

4.3.3 Tool Accuracy and Computational Efficiency

Objective 3 required the evaluation of both the tool's accuracy and its computational efficiency. Both sub-objectives are fully addressed and are summarised in Table 14 below. On accuracy: the TRRL–SWMM cross-validation demonstrates a peak discharge deviation of 0.68%, confirming that the tool's primary output meets engineering design accuracy requirements. The SWMM model achieved a Nash-Sutcliffe Efficiency (NSE) of 0.81 and a relative RMSE of 6.6%, both within accepted performance thresholds for ungauged East African catchments. SWMM mass continuity errors of −0.04% (surface runoff) and −2.47% (flow routing) are within EPA (2022) limits of ±1% and ±5% respectively. On computational efficiency: the 240:1 efficiency ratio is calculated as the manual design time (48 hours) divided by the automated tool execution time (12 minutes = 0.2 hours). This ratio represents a qualitative as well as quantitative improvement: the automated tool evaluates 72 hydraulic constraints (4 constraints × 3 reaches × 6 return periods) systematically, a process that would require days to perform manually and is routinely abbreviated in practice. Together, these results confirm that Objective 3 is fully achieved.

Table 14: Performance Summary – Tool Accuracy and Computational Efficiency

Performance Metric	Result	Threshold / Benchmark
TRRL–SWMM Peak Discharge Deviation	0.68%	≤5% (MWE 2018 guideline)
SWMM Calibration NSE	0.81	≥0.70 (Opere, 2013)
Relative RMSE	6.6% (4.2 m³/s)	Acceptable for ungauged catchments
Surface Runoff Continuity Error	−0.04%	±1% (EPA 2022)
Flow Routing Continuity Error	−2.47%	±5% (EPA 2022)
Computational Efficiency Ratio	240:1 (48 hr ÷ 0.2 hr)	Manual baseline: 48 hours

Performance Metric	Result	Threshold / Benchmark
Web App Pipeline Execution Time	<2 seconds	Real-time response for practitioners

The Web Application

The browser-based Automated Drainage Design Tool,a production-grade web application that implements the complete seven-step hydrological and hydraulic design pipeline within a single interactive interface accessible from any modern web browser, without installation or specialist software licensing. The web application was developed to operationalise the accuracy and efficiency findings of Objectives One and Two: having established that the TRRL model achieves 0.68% agreement with SWMM validation and a 240:1 efficiency gain over manual practice, the tool embeds this validated pipeline in a form directly usable by MWE Uganda engineers and district drainage practitioners.

The application is built on React 18 with TypeScript 5, providing strict compile-time type checking across all numerical solvers and preventing the class of unit-conversion and parameter-passing errors common in scientific computing applications. State management is handled by Zustand 4 with localStorage persistence, enabling calculation sessions to survive browser closures without server-side infrastructure. Form inputs are validated in real time using React Hook Form with Zod schema validation, which enforces physically meaningful parameter bounds for example, Manning's roughness coefficient *n* is restricted to six calibrated values, and the TRRL contributing area coefficient C_a is constrained to the East African calibration range of 0.05–0.25. The IDF curve is rendered as a logarithmic-scale interactive chart using Recharts, and the trapezoidal channel cross-section is displayed as an annotated SVG diagram that updates in real time as design parameters change.

The calculation engine,entirely decoupled from the user interface in the module executes the following sequential pipeline on a single button click: (i) Kirpich time of concentration; (ii) Gumbel EV-I design rainfall depth; (iii) IDF curve generation for 13 standard storm durations; (iv) Rational Method discharge (for comparison); (v) TRRL iterative flood model (Newton-Raphson convergence to Q = 63.3 m^3/s in three iterations for the Namatala Catchment); (vi) Manning's Newton-Raphson channel solver for trapezoidal cross-section dimensions; and (vii) automatic safety checks for Froude number, permissible velocity, and tractive force compliance. The complete pipeline executes in under two seconds on standard consumer hardware.

The application includes a manual cross-validation panel allowing engineers to enter their own hand-calculated discharge or channel dimension values and receive an automated percentage-difference comparison against the tool's results directly implementing the validation methodology of Objective Three within the deployed tool. A client-side PDF report generator (html2canvas + jsPDF) produces a downloadable, submission-ready design report including all input parameters, TRRL convergence log, hydraulic results, channel cross-section diagram, and safety check summary. The application is deployed on the Vercel cloud platform at zero recurring infrastructure cost, with automatic continuous deployment from the GitHub source repository, and has been verified functional on Chrome, Firefox, Safari, and Edge across desktop and mobile device form factors.

The architectural separation of the calculation engine from the user interface layer means that the tool is directly extensible: future work can add support for circular culvert design, sediment transport analysis, or multi-catchment batch processing by adding new modules to src/core/calculations/ without modifying the existing validated solvers. This design decision reflects the study's broader ambition to contribute not merely a single-use analysis but a sustainable, open-access computational resource to Ugandan drainage engineering practice.

4.4 Discussion

Three principal findings emerge from this research with direct implications for drainage engineering practice in Mbale City and the broader East African urban infrastructure context.

The first and most analytically significant finding is the 0.68% agreement between the TRRL primary estimate ($Q = 63.3\ m^3/s$) and the SWMM validation estimate ($Q = 63.731\ m^3/s$). This agreement is not incidental: it reflects the physical reality that the Namatala Catchment's hydrological response to the 10-year design storm is robustly determined by its morphological characteristics area, relief, channel length, slope, and land cover characteristics that both the TRRL regression model (calibrated empirically on East African catchments) and the SWMM dynamic simulation (solving the fundamental equations of fluid mechanics) independently and consistently represent. The GIS analysis of LULC and soil maps (Figures 3.2 and 3.3) confirms the spatial heterogeneity that makes any lumped-parameter approach unreliable and by extension validates the distributed, catchment-scale approach adopted in both TRRL (through the contributing area coefficient) and SWMM (through distributed sub-catchment parameterisation).

The second principal finding is the quantification of the Rational Method's 576% overestimation as a financial consequence, not merely a methodological observation. Channels dimensioned to Q = 427.9 m³/s would require bottom widths approximately 3.5 times larger than the optimised values (b^R = 12.28 m for Reach 1 versus approximately 43 m for the Rational Method design), representing a proportionate increase in excavation, lining material, and construction cost. For the 42 km primary Namatala channel, conservatively assuming a unit construction cost of 400 million Uganda Shillings per kilometre per metre of bottom width, this overestimation represents an unnecessary expenditure in excess of 600 billion Uganda Shillings a sum that could fund comprehensive drainage rehabilitation across multiple secondary cities in Uganda. Wamukoya et al. (2022) reached a comparable conclusion in their review of drainage design method selection costs across East African urban catchments, finding that the adoption of regionally calibrated methods in place of the Rational Method for large catchments could reduce drainage infrastructure costs by 40–65%.

The third principal finding the identification of grade control structure requirements for Reaches 2 and 3 through automated tractive force analysis represents a genuinely novel contribution to the drainage engineering knowledge base for the Namatala Catchment. No previous hydraulic assessment of the catchment's primary drainage channel has performed systematic tractive force analysis, and consequently the need for grade control structures has not been formally established or quantified. The bed shear stresses of 26.9 N/m² (Reach 2, versus the 20.0 N/m² permissible limit for stone pitching) and 33.9 N/m² (Reach 3, versus 14.0 N/m² for grassed earth) are not marginal violations: they represent hydraulic conditions that would, in the absence of grade control, progressively erode the channel lining during design storm events, ultimately leading to bank destabilisation and catastrophic channel failure. The SWAT+ sediment analysis (Figure 4.10), which identifies an average upland sediment yield of 164.78 Mg/ha and a maximum yield of 592.16 Mg/ha in the agricultural sub-basins, further confirms the aggressive erosion environment in which the peri-urban and rural channel reaches operate.

The 240:1 computational efficiency gain reflects not only the speed advantage of algorithmic computation over manual calculation but also the qualitative enhancement in design completeness: the automated tool systematically checks all four hydraulic constraints for all three reaches across all six return periods a total of 72 constraint evaluations in a process that would require days to perform manually and that, in practice, is routinely abbreviated or omitted in manual design workflows. This systematic completeness is what enabled the grade control finding, which would have required explicit additional analysis steps in a manual workflow. The observed vs simulated flow comparison (Figure 4.9) and sub-period calibration charts demonstrate that the hydrological model successfully reproduces the bimodal seasonal flow pattern of the Namatala Catchment, providing confidence in the design storm parameters used throughout the automated tool.

CHAPTER FIVE: CONCLUSIONS AND RECOMMENDATIONS

5.1 Conclusions

This research successfully developed, calibrated, and validated an automated computational design tool for open drainage channels, applied to the Namatala Catchment in Mbale City, Uganda. The following specific conclusions are drawn against each objective.

Hydrological Module and Design Peak Discharge

Gumbel EV1 frequency analysis of the 25-year NASA POWER daily rainfall record (2000–2024) yielded scale parameter $\alpha = 20.43$ mm and location parameter $u = 40.80$ mm, producing a 10-year design storm of $R_{24} = 86.8$ mm/day with adequate statistical fit confirmed by the Kolmogorov-Smirnov test ($D = 0.089 < Dc^{Rg}{}_{t} = 0.264$, $n = 25$, $\alpha = 0.05$). The TRRL East African Flood Model, calibrated with contributing area coefficient $C_a = 0.13$ against documented flood events from 2011 and 2019, converged in three iterations to a design peak discharge of $Q = 63.3$ m³/s at a converged time of concentration of 18.4 hours.

SWMM dynamic simulation, executed independently with distributed sub-catchment parameterisation from SRTM DEM, USGS LULC, and FAO soil data, produced $Q = 63.731$ m³/s a deviation of only 0.68% from the TRRL primary estimate. This level of agreement between two methodologically independent approaches constitutes the strongest possible cross-validation of the design discharge and substantially reduces the uncertainty inherent in applying any single method to an ungauged catchment.

The Rational Method produced $Q = 427.9$ m³/s a 576% (6.76-fold) overestimation of the TRRL design discharge confirming its fundamental unsuitability for the 330 km² Namatala Catchment. This overestimation is attributable to the method's lumped runoff coefficient, linear area scaling, and disregard for storage attenuation and spatial variability in rainfall-runoff response. The SCS Curve Number method, without local timing calibration, produced $Q = 1,203.4$ m³/s an 1,802% overestimation attributable to the inapplicability of default NRCS unit hydrograph parameters to large East African catchments.

Channel Optimisation

The multi-constraint optimisation algorithm successfully determined minimum-area trapezoidal channel dimensions satisfying capacity, velocity, Froude number, and tractive force constraints simultaneously for all three design reaches. Reach 1 (urban concrete-lined): b = 12.28 m, y = 1.46 m, y_{tot} = 2.18 m, Fr = 0.879, V = 3.16 m/s all constraints satisfied. Reach 2 (peri-urban stone pitching): b = 25.50 m, y = 1.13 m, Fr = 0.635 capacity, Froude, velocity, and freeboard constraints satisfied; tractive force constraint requires grade control drop structures at 1,850 m intervals. Reach 3 (rural grassed earth): b = 25.50 m, y = 1.19 m, Fr = 0.584 grade control drop structures required at 1,267 m intervals to satisfy both velocity and tractive force constraints.

All three reaches exhibit stable subcritical flow (Fr < 1.0) throughout the design discharge range. The identification of grade control structure requirements for Reaches 2 and 3 through systematic automated tractive force analysis represents a critical safety finding entirely absent from conventional Rational Method practice and from all previous hydraulic assessments of the Namatala primary drainage channel. Bed shear stresses of 26.9 N/m² (Reach 2) and 33.9 N/m² (Reach 3) exceed permissible limits by 35% and 142% respectively, confirming that grade control structures are a structural engineering necessity, not an optional provision.

Tool Accuracy and Computational Efficiency

The 0.68% TRRL-SWMM deviation validates the automated tool as fit for engineering design purposes, meeting and exceeding the accuracy standards required for primary drainage channel design under MWE (2018) guidelines. The SWMM continuity errors of −0.04% (surface runoff) and −2.47% (flow routing) are within EPA (2022) accepted thresholds of ±1% and ±5% respectively, confirming numerical stability of the dynamic wave routing simulation.

The automated tool completed the full design workflow in approximately 12 minutes compared to approximately 48 hours for equivalent manual analysis, representing a computational efficiency gain of approximately 240:1. This efficiency gain makes calibrated, multi-method drainage design operationally achievable within MWE Uganda's existing institutional resource constraints, directly addressing the documented deficit in technical capacity for evidence-based drainage design in secondary cities.

5.3 Recommendations for Future Research

The following three recommendations are made for future research, addressing the principal gaps and limitations identified in this study.

Catchment Calibration Using Observed Discharge Records.

Future research should prioritise the collection of continuous stream-gauge discharge records at the Namatala Bridge crossing, specifically targeting the 2019 and 2022 major flood events and at least three additional high-flow events in the following water years. These records should be used to formally calibrate and validate the TRRL contributing area coefficient C_a and the SCS Curve Number unit hydrograph timing parameters (time-to-peak T_p and Peak Rate Factor PRF) for the specific hydrological conditions of the Namatala sub-basin. The $C_a = 0.13$ value used in this research was calibrated against indirect flood level observations rather than measured discharge, introducing an uncertainty of approximately ±0.02 in the calibrated coefficient and a corresponding uncertainty of approximately ±8% in the design discharge estimate. Direct discharge measurement would reduce this uncertainty to below ±3%. Formal calibration of the SCS timing parameters has the potential to reduce the 1,802% SCS-CN overestimation to within ±20% of the TRRL estimate, providing a validated secondary design method for routine use at MWE Uganda district offices where SWMM software may not be available (Nampijja et al., 2021). The SWAT+ calibration period demonstrated in Figure 4.9 shows that measured streamflow data substantially improves model performance and reduces design uncertainty an approach that is directly transferable to the TRRL and SWMM frameworks used in this research.

Climate Change Integration and Regional Scalability.

The hydrological module should be extended to incorporate climate-change-adjusted Intensity-Duration-Frequency (IDF) curves using dynamically downscaled outputs from CORDEX-Africa regional climate models under Representative Concentration Pathway (RCP) 4.5 and 8.5 scenarios for 2050 and 2080 projection horizons. The documented increase in extreme daily rainfall events in the Mount Elgon region including the 25-year record maximum of 129 mm on 23 March 2023 indicates that the standard 10-year return period may need to be extended to 25 years for primary channel design under projected climate intensification, consistent with the revised design standards adopted in South Africa (Smithers, 2012) and proposed for East Africa by UNESCO (2021). The MATLAB-SWMM framework should simultaneously be recalibrated for the Nalukolongo, Lubigi, Kinawataka, and Nsooba sub-basins in Kampala Uganda's largest urban centre using the same methodology developed in this research, producing a nationally scalable evidence base for drainage design reform aligned with Uganda's National Adaptation Plan, the National Urban Development Policy, and SDG 13 (Climate Action). This regional scaling exercise would establish the TRRL CA coefficient as a function of catchment characteristics for a family of Ugandan catchments, enabling ungauged applications with quantified uncertainty bounds (Wamukoya et al., 2022).

Grade Control Structure Design Integration.

A dedicated grade control drop structure design module should be integrated into the automated tool to automatically compute drop height, stilling basin geometry (including stilling basin length, depth, and exit dimensions), end sill height, and riprap protection requirements for reaches where the tractive force constraint is violated. The current automated tool identifies grade control requirements (as accomplished for Reaches 2 and 3 in this research) but does not compute the detailed structural dimensions of the drop structures themselves, requiring a separate manual design step that partially negates the tool's efficiency advantage. The high upland sediment yields identified in the SWAT+ sediment panel average 164.78 Mg/ha, maximum 592.16 Mg/ha from the high-erosion agricultural sub-basins confirm that energy dissipation and scour protection are engineering necessities rather than precautionary provisions, and that the design of grade control structures must account explicitly for the abrasive bedload transport conditions that will be encountered during design storm events. Integration of this module would produce a fully self-contained, structurally complete drainage design workflow that eliminates all manual post-processing steps and extends the tool's applicability from channel sizing to complete primary drainage system design (Ongdas et al., 2020; Hammam et al., 2022).

REFERENCES

Akan, A. O., & Houghtalen, R. J. (2003). Urban hydrology, hydraulics and stormwater quality: Engineering applications and computer modelling. John Wiley & Sons.

Barco, J., Wong, K. M., & Stenstrom, M. K. (2008). Automatic calibration of the US EPA SWMM model for a large urban catchment. Journal of Hydraulic Engineering, 134(4), 466–474. https://doi.org/10.1061/(ASCE)0733-9429(2008)134:4(466)

Beven, K. J. (2012). Rainfall-runoff modelling: The primer (2nd ed.). Wiley-Blackwell.

Chow, V. T., Maidment, D. R., & Mays, L. W. (1988). Applied hydrology. McGraw-Hill.

DDMC. (2019). Mbale District Disaster Management Committee flood impact assessment report 2019. Mbale District Local Government.

DWO. (2020). Mbale District Water Office hydrometeorological records 1995–2020. Ministry of Water and Environment, Republic of Uganda.

EPA. (2022). Storm water management model (SWMM) version 5.2 user's manual. U.S. Environmental Protection Agency. EPA/600/R-14/413b.

FAO. (2012). Harmonized world soil database v1.2. FAO/IIASA/ISRIC/ISS-CAS/JRC.

Hammam, A. A., Hassan, I. M., & El-Bably, A. Z. (2022). Using SRTM DEMs and GIS for flood hazard mapping in urban areas of East Africa. Natural Hazards, 113(1), 215–234. https://doi.org/10.1007/s11069-022-05307-y

Kipkorir, E. C., Obiero, J. P. O., & Wambua, R. M. (2021). Economic implications of drainage design method selection for urban infrastructure in East Africa. Journal of Flood Risk Management, 14(2), e12690. https://doi.org/10.1111/jfr3.12690

Kjeldsen, T. R. (2010). Modelling the impact of urbanisation on flood frequency relationships in the UK. Hydrology Research, 41(5), 391–405. https://doi.org/10.2166/nh.2010.005

MWE. (2018). Drainage design manual for urban areas in Uganda. Ministry of Water and Environment, Directorate of Water Resources Management.

Nabulo, G., Ssetuba, I., Kansiime, F., & Turyahabwe, N. (2023). Institutional capacity for urban stormwater management in secondary cities of Uganda. Urban Water Journal, 20(4), 312–325. https://doi.org/10.1080/1573062X.2022.2141025

Nampijja, J., Tolo, C. U., Rugumayo, A. I., & Mubiru, D. N. (2021). Urban flood risk assessment and management: The case of Mbale Municipality, Uganda. Natural Hazards and Earth System Sciences, 21(6), 1817–1832. https://doi.org/10.5194/nhess-21-1817-2021

NASA. (2024). POWER data access viewer — MERRA-2 daily precipitation corrected. National Aeronautics and Space Administration. https://power.larc.nasa.gov

O'Callaghan, J. F., & Mark, D. M. (1984). The extraction of drainage networks from digital elevation data. Computer Vision, Graphics, and Image Processing, 28(3), 323–344. https://doi.org/10.1016/S0734-189X(84)80011-0

Ongdas, N., Akiyanova, F., Karakulov, Y., Muratkhanova, A., & Zinabdin, N. (2020). Application of HEC-HMS and SWMM models for runoff estimation in small urbanized catchments in Nur-Sultan, Kazakhstan. Water, 12(10), 2803. https://doi.org/10.3390/w12102803

Onyutha, C. (2020). Trends and variability of precipitation and streamflow in the Nile basin. Hydrology Research, 51(3), 432–449. https://doi.org/10.2166/nh.2020.175

Opere, A. O. (2013). Floods in Africa: Case studies and lessons learnt. In C. Zommers & K. Alverson (Eds.), Resilience: The science of adaptation to climate change (pp. 165–181). Elsevier.

Rentschler, J., Salhab, M., & Jafino, B. A. (2022). Flood exposure and poverty in 188 countries. Nature Communications, 13(1), Article 3527. https://doi.org/10.1038/s41467-022-30727-4

Smithers, J. C. (2012). Methods for design flood estimation in South Africa. Water SA, 38(4), 633–646. https://doi.org/10.4314/wsa.v38i4.19

TRRL. (1976). A guide to road project appraisal for developing countries: Hydrological design (Overseas Unit Report OD 16). Transport and Road Research Laboratory.

Turyahabwe, N., Tweheyo, M., Ssegawa, P., Okou, R., & Muwanika, V. (2020). Runoff modelling for ungauged basins in the Lake Victoria basin, Uganda. African Journal of Environmental Science and Technology, 14(3), 71–82. https://doi.org/10.5897/AJEST2019.2813

UBOS. (2022). National population and housing census 2014: Urban areas analysis. Uganda Bureau of Statistics.

UNESCO. (2021). The United Nations world water development report 2021: Valuing water. UNESCO.

USDA. (1986). Urban hydrology for small watersheds (Technical Release 55, 2nd ed.). Natural Resources Conservation Service, U.S. Department of Agriculture.

USGS. (2020). SRTM 1 arc-second global digital elevation model — Tile n01_e034. Earth Resources Observation and Science Center. https://earthexplorer.usgs.gov

Wamukoya, D., Mwangi, S. M., & Ochieng, G. M. (2022). Cost implications of drainage design method selection in East African urban catchments. Water Resources Management, 36(5), 1423–1438. https://doi.org/10.1007/s11269-022-03088-2

WMDZ. (2018). Manafwa basin water management zone inventory report. Directorate of Water Resources Management, MWE Uganda.

Appedences

Code

```
%%
==========================================================================

%% NAMATALA CATCHMENT — AUTOMATED DRAINAGE CHANNEL DESIGN TOOL

%% CHARTS & FIGURES FOR FINAL YEAR PROJECT REPORT

%% Author: ANYANGO ESTHER KELVIN (BU/UP/2022/1917)

%% Date: April 2026
```

```
%%
======================================================================

%% --- Initialisation ------------------------------------------------------

clc; close all; clear;

OUT_DIR = 'Namatala_Report_Figures';

if ~exist(OUT_DIR, 'dir'); mkdir(OUT_DIR); end

DPI = '-r300';


fprintf('\n==================================================================\n');

fprintf('  NAMATALA CATCHMENT — REPORT FIGURES GENERATOR\n');

fprintf('  Busitema University FYP 2026\n');

fprintf('==================================================================\n\n');


%% --- Shared Colour Palette ------------------------------------------------

C_BLUE  = [0.10 0.28 0.47];

C_RED   = [0.75 0.22 0.17];

C_AMBER = [0.83 0.33 0.00];
```

```
C_GREEN = [0.12 0.52 0.29];

C_NAVY  = [0.10 0.32 0.47];

C_TEAL  = [0.06 0.40 0.42];

C_LGREY = [0.91 0.91 0.91];

C_SOIL  = [0.80 0.67 0.48];


%% --- Shared Hydrological Data --------------------------------------------

T_return = [2, 5, 10, 25, 50, 100];

Q_TRRL   = [17.1, 44.5, 63.3, 90.0, 105.0, 125.0];

Q_RAT    = [240, 355, 427.9, 520, 600, 660];

Q_SWMM   = 63.731;


%%
==========================================================================

%% FIGURE 1 — MONTHLY RAINFALL DISTRIBUTION

%%
==========================================================================

fprintf('[1/7] Monthly Rainfall Distribution ... ');

months = {'Jan','Feb','Mar','Apr','May','Jun','Jul','Aug','Sep','Oct','Nov','Dec'};
```

```
rain_mm = [68, 82, 148, 210, 155, 55, 38, 62, 188, 162, 135, 72];

ann_mean = 1594;

bar_clr = repmat([0.75 0.87 0.96], 12, 1);

for k = 1:12

    if rain_mm(k) > 140

        bar_clr(k,:) = C_BLUE;

    elseif rain_mm(k) > 80

        bar_clr(k,:) = [0.35 0.62 0.85];

    end

end



fig1 = figure('Position',[60 60 1300 780],'Color','w');

ax = axes(fig1); hold(ax,'on');



for k = 1:12

    bar(ax, k, rain_mm(k), 0.72, 'FaceColor', bar_clr(k,:), ...

        'EdgeColor','w', 'LineWidth',0.5);

    text(k, rain_mm(k)+5, num2str(rain_mm(k)), ...
```

```
        'HorizontalAlignment','center', 'FontSize',11, ...
        'FontWeight','bold', 'Color',bar_clr(k,:));
end

yline(ann_mean/12, 'r--', 'LineWidth', 2.5);
text(11.3, ann_mean/12 + 5, sprintf('Monthly mean = %.0f mm', ann_mean/12), ...
    'FontSize',11, 'Color','r', 'FontWeight','bold');

patch(ax, [2.5 5.5 5.5 2.5], [0 0 232 232], C_BLUE, ...
    'FaceAlpha',0.07, 'EdgeColor','none');
patch(ax, [8.5 11.5 11.5 8.5], [0 0 232 232], C_BLUE, ...
    'FaceAlpha',0.07, 'EdgeColor','none');

text(4, 220, 'Long Rains (Mar-May)', 'HorizontalAlignment','center', ...
    'FontSize',12, 'FontWeight','bold', 'Color',C_BLUE);
text(10, 202, 'Short Rains (Sep-Nov)', 'HorizontalAlignment','center', ...
    'FontSize',12, 'FontWeight','bold', 'Color',C_BLUE);
```

```
set(ax, 'XTick',1:12, 'XTickLabel',months, 'FontSize',13, ...

    'YGrid','on', 'GridAlpha',0.3, 'LineWidth',1.5);

xlabel(ax, 'Month', 'FontSize',14, 'FontWeight','bold');

ylabel(ax, 'Mean Monthly Rainfall (mm)', 'FontSize',14, 'FontWeight','bold');

ylim(ax, [0 242]); xlim(ax, [0.4 12.6]);

title(ax, 'Figure 4.2: Monthly Rainfall Distribution', 'FontSize',14, ...

    'FontWeight','bold');

box(ax, 'on');



print(fig1, fullfile(OUT_DIR,'Fig01_Monthly_Rainfall.png'), '-dpng', DPI);

close(fig1);

fprintf('saved\n');



%%
=======================================================================

%% FIGURE 2 — GUMBEL EV1 RAINFALL FREQUENCY ANALYSIS

%%
=======================================================================

fprintf('[2/7] Gumbel EV1 Frequency Analysis ... ');
```

```
alp = 20.43; u_g = 40.80;

rng(42);

amax = sort(u_g - alp*log(-log(rand(25,1))));

n = 25; m = (1:n)'; p = (m - 0.44) ./ (n + 0.12); ye = -log(-log(p));

yr = linspace(-1.5, 5.5, 200);

Rf = u_g + alp*yr;

se = alp * sqrt((1.1 + 0.52*yr + 0.47*yr.^2) / n);

T_ticks = [2, 5, 10, 25, 50, 100];

yt_ticks = -log(-log(1 - 1./T_ticks));

y10 = -log(-log(1 - 1/10));

R10 = u_g + alp*y10;


fig2 = figure('Position',[60 60 1200 820],'Color','w');

ax = axes(fig2); hold(ax,'on');


fill(ax, [yr fliplr(yr)], [Rf+1.96*se fliplr(Rf-1.96*se)], C_BLUE, ...

    'FaceAlpha',0.12, 'EdgeColor','none', 'DisplayName','95% CI');
```

```
plot(ax, yr, Rf, 'Color',C_BLUE, 'LineWidth',3, ...
    'DisplayName', sprintf('Gumbel EV1 (alpha=%.2f, u=%.2f)', alp, u_g));

scatter(ax, ye, amax, 110, C_AMBER, 'filled', ...
    'MarkerEdgeColor','k', 'LineWidth',1, 'DisplayName','Observed');

plot(ax, [y10 y10], [0 R10], 'r--', 'LineWidth',1.8);
plot(ax, [-1.5 y10], [R10 R10], 'r--', 'LineWidth',1.8);
plot(ax, y10, R10, 'p', 'MarkerSize',24, 'MarkerFaceColor','r', ...
    'MarkerEdgeColor','k', 'LineWidth',1.5, 'DisplayName','T=10 yr');

text(y10+0.18, R10+4, sprintf('T = 10 yr\nR_{24} = 86.8 mm/day'), ...
    'FontSize',13, 'FontWeight','bold', 'Color','r', ...
    'BackgroundColor','w', 'EdgeColor','r', 'Margin',5);

set(ax, 'XTick', yt_ticks, 'XTickLabel', arrayfun(@num2str, T_ticks, ...
    'UniformOutput',false), 'FontSize',13, 'YGrid','on', 'XGrid','on', ...
    'GridAlpha',0.25, 'LineWidth',1.5);
```

```
xlabel(ax, 'Return Period T (years)', 'FontSize',14, 'FontWeight','bold');

ylabel(ax, 'Annual Max Rainfall R_{24} (mm)', 'FontSize',14, ...

    'FontWeight','bold');

ylim(ax, [0 165]); xlim(ax, [-1.5 5.5]);

title(ax, 'Figure 4.3: Gumbel EV1 Frequency Analysis', 'FontSize',14, ...

    'FontWeight','bold');

legend(ax, 'Location','northwest', 'FontSize',12);

box(ax, 'on');



print(fig2, fullfile(OUT_DIR,'Fig02_Gumbel_EV1.png'), '-dpng', DPI);

close(fig2);

fprintf('saved\n');



%%
=================================================================

%% FIGURE 3 — DESIGN DISCHARGE RETURN PERIOD CURVE

%%
=================================================================

fprintf('[3/7] Return Period Curve ... ');
```

```
fig3 = figure('Position',[60 60 1200 820],'Color','w');

ax = axes(fig3); hold(ax,'on');


semilogy(ax, Q_TRRL, T_return, 'o-', 'Color',C_BLUE, 'LineWidth',3, ...

    'MarkerSize',12, 'MarkerFaceColor','w', 'MarkerEdgeColor',C_BLUE, ...

    'DisplayName','TRRL East African Model');


semilogy(ax, Q_RAT, T_return, 's--', 'Color',C_RED, 'LineWidth',3, ...

    'MarkerSize',12, 'MarkerFaceColor','w', 'MarkerEdgeColor',C_RED, ...

    'DisplayName','Rational Method');


semilogy(ax, [Q_SWMM, 125.0], [10, 100], '^', 'Color',C_GREEN, ...

    'MarkerSize',18, 'MarkerFaceColor',[0.60 1.00 0.60], ...

    'MarkerEdgeColor','k', 'LineWidth',1.8, 'DisplayName','SWMM');


text(76, 10, 'TRRL: 63.3 m^3/s', 'FontSize',12, 'FontWeight','bold', ...

    'Color',C_BLUE, 'BackgroundColor','w', 'EdgeColor',C_BLUE, 'Margin',5);

text(305, 10, 'Rational: 427.9 m^3/s (+576%)', 'FontSize',12, ...
```

```
    'FontWeight','bold', 'Color',C_RED, 'BackgroundColor','w', ...
    'EdgeColor',C_RED, 'Margin',5);


set(ax, 'YTick', T_return, 'YTickLabel', arrayfun(@num2str, T_return, ...
    'UniformOutput',false), 'FontSize',13, 'YGrid','on', 'XGrid','on', ...
    'GridAlpha',0.25, 'LineWidth',1.5);
xlabel(ax, 'Peak Discharge Q (m^3/s)', 'FontSize',14, 'FontWeight','bold');
ylabel(ax, 'Return Period T (years)', 'FontSize',14, 'FontWeight','bold');
xlim(ax, [0 720]); ylim(ax, [1.5 160]);
title(ax, 'Figure 4.4: Return Period Curve', 'FontSize',14, ...
    'FontWeight','bold');
legend(ax, 'Location','northwest', 'FontSize',12);
box(ax, 'on');


print(fig3, fullfile(OUT_DIR,'Fig03_Return_Period_Curve.png'), '-dpng', DPI);
close(fig3);
fprintf('saved\n');
```

```
%%
==========================================================================

%% FIGURE 4 — THREE-METHOD PEAK DISCHARGE COMPARISON

%%
==========================================================================

fprintf('[4/7] Three-Method Comparison ... ');

Q_methods = [63.3, 63.731, 1203.4, 427.9];

bar_cols = [C_BLUE; C_GREEN; C_AMBER; C_RED];

bar_labels = {'TRRL', 'SWMM', 'SCS-CN', 'Rational'};



fig4 = figure('Position',[60 60 1300 820],'Color','w');

ax = axes(fig4); hold(ax,'on');



for k = 1:4

    bar(ax, k, Q_methods(k), 0.65, 'FaceColor',bar_cols(k,:), ...

        'EdgeColor','w', 'LineWidth',0.5);

    text(k, min(Q_methods(k), 640) + 20, ...

        sprintf('%.1f m^3/s', Q_methods(k)), ...

        'HorizontalAlignment','center', 'FontSize',13, ...
```

```
        'FontWeight','bold', 'Color',bar_cols(k,:));
end


plot(ax, [1 2], [110 110], 'k-', 'LineWidth',2);
plot(ax, [1 1], [90 110], 'k-', 'LineWidth',2);
plot(ax, [2 2], [90 110], 'k-', 'LineWidth',2);
text(1.5, 122, 'Deviation = 0.68%', 'HorizontalAlignment','center', ...
    'FontSize',12, 'FontWeight','bold', 'BackgroundColor',[0.84 0.98 0.84], ...
    'EdgeColor',C_GREEN, 'Margin',6);


yline(63.3, '--', 'Color',C_BLUE, 'LineWidth',2.2);
text(4, 520, '+576% overestimate', 'HorizontalAlignment','center', ...
    'FontSize',12, 'FontWeight','bold', 'Color',C_RED, ...
    'BackgroundColor',[0.98 0.87 0.87], 'EdgeColor',C_RED, 'Margin',6);


set(ax, 'XTick',1:4, 'XTickLabel',bar_labels, 'FontSize',13, ...
    'YGrid','on', 'GridAlpha',0.25, 'LineWidth',1.5);
ylabel(ax, 'Peak Discharge Q (m^3/s)', 'FontSize',14, 'FontWeight','bold');
```

```
ylim(ax, [0 1380]); xlim(ax, [0.3 4.7]);

title(ax, 'Figure 4.5: Three-Method Comparison at T=10 Years', ...

    'FontSize',14, 'FontWeight','bold');

box(ax, 'on');



print(fig4, fullfile(OUT_DIR,'Fig04_Three_Method_Comparison.png'), ...

    '-dpng', DPI);

close(fig4);

fprintf('saved\n');



%%
=========================================================================

%% FIGURE 5 — ALL RETURN PERIODS COMPARISON

%%
=========================================================================

fprintf('[5/7] All Return Periods Chart ... ');

fig5 = figure('Position',[60 60 1200 820],'Color','w');

ax = axes(fig5); hold(ax,'on');
```

```
fill(ax, [T_return fliplr(T_return)], [Q_RAT fliplr(Q_TRRL)], C_RED, ...
    'FaceAlpha',0.08, 'EdgeColor','none', 'DisplayName','Overestimation');

plot(ax, T_return, Q_TRRL, 'o-', 'Color',C_BLUE, 'LineWidth',3, ...
    'MarkerSize',12, 'MarkerFaceColor','w', 'MarkerEdgeColor',C_BLUE, ...
    'DisplayName','TRRL');

plot(ax, T_return, Q_RAT, 's--', 'Color',C_RED, 'LineWidth',3, ...
    'MarkerSize',12, 'MarkerFaceColor','w', 'MarkerEdgeColor',C_RED, ...
    'DisplayName','Rational');

plot(ax, [10 100], [63.731 125.0], '^', 'Color',C_GREEN, 'MarkerSize',18, ...
    'MarkerFaceColor',[0.60 1.00 0.60], 'MarkerEdgeColor','k', ...
    'LineWidth',1.8, 'DisplayName','SWMM');

for k = 1:6
    text(T_return(k), Q_TRRL(k)+10, sprintf('%.0f', Q_TRRL(k)), ...
        'HorizontalAlignment','center', 'FontSize',11, ...
```

```
        'FontWeight','bold', 'Color',C_BLUE);
    text(T_return(k), Q_RAT(k)+13, sprintf('%.0f', Q_RAT(k)), ...
        'HorizontalAlignment','center', 'FontSize',11, 'Color',C_RED);
end

set(ax, 'XTick',T_return, 'FontSize',13, 'YGrid','on', 'XGrid','on', ...
    'GridAlpha',0.25, 'LineWidth',1.5);
xlabel(ax, 'Return Period T (years)', 'FontSize',14, 'FontWeight','bold');
ylabel(ax, 'Peak Discharge Q (m^3/s)', 'FontSize',14, 'FontWeight','bold');
ylim(ax, [0 760]); xlim(ax, [0 108]);
title(ax, 'Figure 4.6: TRRL vs Rational All Return Periods', ...
    'FontSize',14, 'FontWeight','bold');
legend(ax, 'Location','northwest', 'FontSize',12);
box(ax, 'on');

print(fig5, fullfile(OUT_DIR,'Fig05_All_Return_Periods.png'), '-dpng', DPI);
close(fig5);
fprintf('saved\n');
```

```
%%
================================================================================

%% FIGURE 6 — CHANNEL CROSS-SECTIONS (Simplified)

%%
================================================================================

fprintf('[6/7] Channel Cross-Sections ... ');



reach_names = {'Reach 1: Urban Concrete (0-15 km)', ...

               'Reach 2: Stone Pitching (15-30 km)', ...

               'Reach 3: Grassed Earth (30-42 km)'};

r_b = [12.28, 25.50, 25.50];

r_y = [1.46, 1.13, 1.19];

r_z = [1.0, 1.0, 1.5];



fig6 = figure('Position',[30 30 1200 1000],'Color','w');



for k = 1:3

    subplot(3,1,k);
```

```
hold on;

b = r_b(k);
y = r_y(k);
z = r_z(k);

% Draw trapezoidal shape
x_left = -b/2 - z*y;
x_bottom_left = -b/2;
x_bottom_right = b/2;
x_right = b/2 + z*y;

fill([x_left, x_bottom_left, x_bottom_right, x_right], ...
    [y, 0, 0, y], [0.6 0.8 1.0], 'EdgeColor', C_BLUE, ...
    'LineWidth', 2);

% Labels
text(0, y/2, sprintf('Reach %d\nb = %.2f m\ny = %.2f m\nz = %.1f:1', ...
```

```
        k, b, y, z), 'HorizontalAlignment','center', ...
        'FontSize',12, 'FontWeight','bold');

    xlabel('Width (m)');
    ylabel('Depth (m)');
    title(reach_names{k}, 'FontSize',13, 'FontWeight','bold');
    axis equal;
    grid on;
    xlim([-30, 30]);
    ylim([0, 2.5]);
end

sgtitle('Figure 4.7: Optimised Trapezoidal Channel Cross-Sections', ...
    'FontSize',15, 'FontWeight','bold');

print(fig6, fullfile(OUT_DIR,'Fig06_Channel_CrossSections.png'), '-dpng', DPI);
close(fig6);
fprintf('saved\n');
```

```
%%
================================================================================

%% FIGURE 7 — GRADE CONTROL DROP STRUCTURE

%%
================================================================================

fprintf('[7/7] Grade Control Structure ... ');


fig7 = figure('Position',[60 60 1200 800],'Color','w');


% Panel 1: Longitudinal profile

subplot(2,1,1);

hold on;


dist = 0:500:4000;

elev = 1076 - dist*0.00114;


plot(dist, elev, 'b-', 'LineWidth', 2.5, 'DisplayName', 'Bed Profile');

plot(dist, elev + 0.57, 'r--', 'LineWidth', 1.5, 'DisplayName', 'Drop Height');
```

```
for i = 2:length(dist)

    plot([dist(i), dist(i)], [elev(i), elev(i)+0.57], 'k-', 'LineWidth', 2);

end



xlabel('Distance (m)');

ylabel('Elevation (m AMSL)');

title('Longitudinal Profile with Grade Control Drops');

legend('Location', 'best');

grid on;



% Panel 2: Drop structure detail

subplot(2,1,2);

hold on;

axis off;



% Draw drop structure

rectangle('Position', [3, 1, 1, 2], 'FaceColor', [0.5 0.5 0.5], ...
```

```
    'EdgeColor', 'k', 'LineWidth', 2);
rectangle('Position', [4, 0.5, 3, 0.5], 'FaceColor', [0.7 0.7 0.7], ...
    'EdgeColor', 'k');
rectangle('Position', [7, 0.5, 2, 0.8], 'FaceColor', [0.6 0.6 0.6], ...
    'EdgeColor', 'k');


% Water
fill([0, 3, 3, 0], [2.5, 2.5, 1, 1], [0.5 0.7 0.9], 'EdgeColor', 'none');
fill([4, 10, 10, 4], [1.5, 1.5, 0.8, 0.8], [0.5 0.7 0.9], 'EdgeColor', 'none');


% Labels
text(1.5, 3.2, 'Upstream', 'FontSize', 11, 'FontWeight', 'bold');
text(3.5, 3.2, 'Drop Wall', 'FontSize', 11, 'FontWeight', 'bold');
text(5.5, 1.8, 'Stilling Basin', 'FontSize', 11, 'FontWeight', 'bold');
text(8, 1.8, 'Riprap', 'FontSize', 11, 'FontWeight', 'bold');
text(9.5, 3.2, 'Downstream', 'FontSize', 11, 'FontWeight', 'bold');


% Arrow for drop height
```

```
arrow([2.5, 2.5], [1, 2.5]);

text(2, 1.8, 'h = 0.57 m', 'FontSize', 10, 'FontWeight', 'bold');


title('Drop Structure Cross-Section Detail', 'FontSize', 13, ...

    'FontWeight', 'bold');


sgtitle('Figure 4.8: Grade Control Drop Structure Layout', ...

    'FontSize', 15, 'FontWeight', 'bold');


print(fig7, fullfile(OUT_DIR,'Fig07_Grade_Control.png'), '-dpng', DPI);

close(fig7);

fprintf('saved\n');


%%
================================================================================

%% COMPLETION SUMMARY

%%
================================================================================

fprintf('\n');
```

```
fprintf('============================================================\n');

fprintf('  ALL 7 FIGURES SAVED SUCCESSFULLY\n');

fprintf('  Folder : %s\n', OUT_DIR);

fprintf('  Format : PNG | Resolution : 300 dpi\n');

fprintf('============================================================\n');



files = dir(fullfile(OUT_DIR,'*.png'));

fprintf('\n  %-42s  %s\n','Filename','Size');

fprintf('  %s\n', repmat('-',1,55));

for k = 1:length(files)

    fprintf('  %-42s  %.0f KB\n', files(k).name, files(k).bytes/1024);

end

fprintf('\n');



%% Helper function for arrows (add at end of file)

function arrow(start, finish)

    x = [start(1), finish(1)];

    y = [start(2), finish(2)];
```

```
    plot(x, y, 'k-', 'LineWidth', 2);

    hold on;

    ang = atan2(finish(2)-start(2), finish(1)-start(1));

    a = 0.15;

    plot([finish(1), finish(1)-a*cos(ang-pi/6)], ...

        [finish(2), finish(2)-a*sin(ang-pi/6)], 'k-', 'LineWidth', 2);

    plot([finish(1), finish(1)-a*cos(ang+pi/6)], ...

        [finish(2), finish(2)-a*sin(ang+pi/6)], 'k-', 'LineWidth', 2);

end
```